Study on the monitoring method of cavity growth in underground coal gasification under laboratory conditions

Su, Fa-qiang
School of Energy Science and Engineering, Henan Polytechnic University

Wu, Jun-bo
School of Energy Science and Engineering, Henan Polytechnic University

Zhang, Tao
School of Energy Science and Engineering, Henan Polytechnic University

Deng, Qi-chao
School of Energy Science and Engineering, Henan Polytechnic University

他

出版情報：Energy. 263 (Part E), pp.126048-, 2023-01-15. Elsevier
バージョン：

Energy

Study on the monitoring method of cavity growth in underground coal gasification under laboratory conditions

--Manuscript Draft--

Manuscript Number:	EGY-D-22-05796R2
Article Type:	Full length article
Keywords:	Underground coal gasification; Combustion cavity; Stratification temperature; Acoustic emission; profile
Corresponding Author:	yihe yu, Ph.D Henan Polytechnic University CHINA
First Author:	Fa-qiang Su, Ph.D
Order of Authors:	Fa-qiang Su, Ph.D
	Jun-bo Wu
	Tao Zhang
	Qi-chao Deng
	yihe yu, Ph.D
	Akihiro Hamanaka
	Meng-Jia Dai
	Jun-Nan Yang
	Xiao-long He
Abstract:	Abstract: The growth state of the combustion cavity during underground coal gasification (UCG) affects the gasification process's efficiency, stability, and accurate monitoring and control. In this study, a simulation experiment of UCG was performed, and a horizontal coaxial gasification channel was drilled based on the constructed artificial coal seam (lump coal). Oxygen and air are used as gasification agents to provide a sufficient temperature field to sustain the gasification process. The effect of different positions of the injection pipe port on the growth of the gasification combustion cavity was studied. Moreover, the derivation of the gasification zone during UCG was developed using stratified temperature monitoring and acoustic emission damage monitoring. After the experiment, the artificial coal seam was cut to obtain the profile shape of the combustion cavity, which was compared with the temperature and acoustic emission monitoring results. The results show that the temperature distribution results in the coal seam and the calibration results of the acoustic emission source during horizontal coaxial UCG are consistent with the two-dimensional and three-dimensional combustion cavities reconstructed by the profile. Thus, the effectiveness of stratified temperature monitoring and acoustic emission monitoring to infer the gasification combustion cavity is proven.

Study on the monitoring method of cavity growth in underground coal gasification under laboratory conditions

Fa-qiang Su[a,b], Jun-bo Wu[a], Tao-Zhang[a], Qi-chao Deng[a], Yi-he Yu[a,b,*], Akihiro Hamanaka[c], Meng-Jia Dai[a], Jun-Nan Yang[a],Xiao-long He[a]

[a] School of Energy Science and Engineering, Henan Polytechnic University, Jiaozuo, Henan, 454-003, China

[b] State Collaborative Innovation Center of Coal Work Safety and Clean-efficiency Utilization, Henan Polytechnic University, Jiaozuo, Henan, 454-003, China

[c] Department of Earth Resources Engineering, Kyushu University, 744 Motooka, Nishi-ku, Fukuoka 819-0395, Japan

* Correspondence: yyhcmsj@hpu.edu.cn

Abstract: The growth state of the combustion cavity during underground coal gasification (UCG) affects the gasification process's efficiency, stability, and accurate monitoring and control. In this study, a simulation experiment of UCG was performed, and a horizontal coaxial gasification channel was drilled based on the constructed artificial coal seam (lump coal). Oxygen and air are used as gasification agents to provide a sufficient temperature field to sustain the gasification process. The effect of different positions of the injection pipe port on the growth of the gasification combustion cavity was studied. Moreover, the derivation of the gasification zone during UCG was developed using stratified temperature monitoring and acoustic emission damage monitoring. After the experiment, the artificial coal seam was cut to obtain the profile shape of the combustion cavity, which was compared with the temperature and acoustic emission monitoring results. The results show that the temperature distribution results in the coal seam and the calibration results of the acoustic emission source during horizontal coaxial UCG are consistent with the two-dimensional and three-dimensional combustion cavities reconstructed by the profile. Thus, the effectiveness of stratified temperature monitoring and acoustic emission monitoring to infer the gasification combustion cavity is proven.

Keywords: Underground coal gasification; Combustion cavity; Stratification temperature; Acoustic emission; Profile

1 Introduction

Underground coal gasification (UCG) is a new type of mining method that involves the process of burning coal stored underground to produce combustible gas in a controlled manner. This process consists of excavating coal from the ground to the coal seam, establishing a gasification channel in the coal seam, injecting gasification agents into the coal seam through the gas injection well, letting the coal go through a series of processes such as oxidation and reduction, and generating gas that is finally discharged to the ground through the production well [1]. During UCG, as gasification progresses, the flow channel between the injection well and the production well expands with the consumption of the coal seam, and the resulting space is called the combustion cavity. Combustion cavity formation is one of the most critical links in the UCG process [2]. The growth of the combustion cavity is a dynamic process; it is the continuous expansion of the gasification channel with combustion and oxidation, accompanied by the generation of many cracks. If the cracks are too large, they may cause excessive damage to the rock strata above the gasification area, and the cracks around the gasification area may also run through the surface or underground water, resulting in gas leakage and environmental pollution and affecting the regular progress of underground coal gasification [3]. For example, in the 1970s and 1980s, dozens of UCG tests were conducted in the United States. Three tests (HoeCreek I, II, and III) at HoeCreek, Wyoming, produced surrounding water pollution and surface subsidence [4-6]. Therefore, monitoring the growth of the combustion cavity during the UCG process is very important for the stability of the upper part of the geological structure and the state of the surrounding environment [7].

Due to the vital role of combustion cavity growth in the UCG process, many scholars have used a variety of modeling methods to study this growth [8-10]. For example, Perkins and Sahajawalla proposed a one-dimensional model to study the effects of different operating parameters on combustion cavity growth in the UCG process, and the results showed that coal characteristics such as temperature, water flow, gas pressure, ash content, and carbon constant value have the most significant influence on the growth rate of the combustion cavity [11]. Luo et al. proposed a two-dimensional mathematical model to study combustion cavity growth in the UCG process, and the results showed that the proposed model could predict the combustion cavity shape, temperature distribution, and amount of gasified coal [12]. Seifi et al. proposed a 3D simulation of the UCG process, which was shown to predict the cavity shape and temperature distribution [13]. Samdani et al. developed a CFD model to simulate the UCG process. In the first stage, when the coal near the injection well is consumed, the cavity grows in the vertical direction, and in the second stage, the cavity grows in the horizontal direction. The results show that the model can predict the combustion cavity growth rate [14-16]. Amin Jowkar et al. introduced the constitutive function equation in simulating UCG. The results show that the constitutive function equation can predict the expansion of the combustion cavity [17]. Eddy et al. established a two-dimensional model to describe the effects of natural convection and forced convection on heat and mass transfer on the sidewall of the combustion cavity [18]. Various research methods based on mathematical models and simulations have revealed the development of combustion cavities. However, some variable factors have been ignored in the simulation, such as the rock and soil mass, which are not homogeneous and isotropic, and the effect of seepage on the temperature field. In addition, coal samples are also heterogeneous, and the UCG process involves complex physical processes, homogeneous and heterogeneous chemical reactions, complex flow patterns of reaction gases, heat and mass transport, and thermal-mechanical failure of coal seams [19]. Moreover, the simulation only considers some specific factors. Thus, the accuracy of the methods cannot be verified since there are no experimental data for comparison.

As a result, some scholars have conducted experiments to analyze the growth rate of combustion cavities. Yang et al. used the transient electromagnetic method to detect the combustion cavity and predicted the boundary of the combustion cavity according to the change law of electrical impedance of coal and surrounding rock under different temperature conditions [20]. Chen et al. predicted the flameworking face's position and the combustion cavity's scope in underground coal gasification by the radioactive radon method. The prediction is mainly based on the enrichment characteristics of radioactive elements in coal before and after combustion and the migration law of radon gas at different temperatures and pressures in the gasification zone [21]. In the underground gasification of the Tangshan Liuzhuang Coal Mine, radioactive radon gas was used to monitor the movement of the gasification working face and the expansion range of the combustion cavity [22]. Mehdi et al. developed a simple model to predict the combustion cavity expansion rate using a nonlinear regression analysis method based on data from UCG field experiments [23]. Prabu et al. designed a gasification device with a special type of wood as a carrier to simulate the expansion of the combustion cavity during the gasification process; however, in this experiment, stopping the gasification process several times and disassembling the model to observe and evaluate the combustion zone was necessary. The results show that the cavity formation rate and cavity shape are significantly affected by the oxidant flow rate [24-25]. Jowkar et al. used COMSOL software to establish a model to predict the combustion cavity's shape and volume and determine the gas's calorific value and composition [26]. Javed et al. parameterized the three-dimensional axisymmetric cavitation simulation model, studied the influence of various operating parameters on the cavitation expansion, and predicted the cavitation expansion and its interaction with overburden [27]. Su et al. used acoustic emission monitoring combined with temperature monitoring and product gas composition analysis to monitor cavity growth during the UCG process [28-29]. In the above studies on the growth of the combustion cavity, the combustion cavity is indirectly inverted by monitoring the signals generated during the UCG process, and there is no direct means to investigate the expansion of the combustion cavity.

In this paper, the underground gasification system of a horizontal coaxial hole-type gasification channel is used to simulate underground coal gasification. In addition, temperature sensors and acoustic emission sensors are arranged in layers to monitor the temperature and acoustic emission signal inside the coal sample during the gasification process. At the end of the experiment, gypsum slurry was filled into the combustion cavity, and after it was solidified and formed, the two-dimensional section morphology of the gasification coal sample was observed layer by layer, and the three-dimensional morphology of the gasification combustion cavity was constructed. Therefore, the variation law of acoustic emission and temperature in the process of gasification combustion cavity expansion is analyzed, and the shape and size of the combustion cavity can be predicted and evaluated based on acoustic emission and temperature monitoring data.

2 UCG experimental model

2.1 UCG experimental system

The UCG experiment was carried out in a steel container filled with large coals. To ensure airtightness, refractory cement was used to fill the voids around the steel container. The UCG simulation experiment system is mainly composed of the main gasifier, the gasification agent injection system, the acoustic emission (AE) monitoring system, the temperature monitoring system, and the product gas analysis system. The schematic diagram is shown in Fig 1.

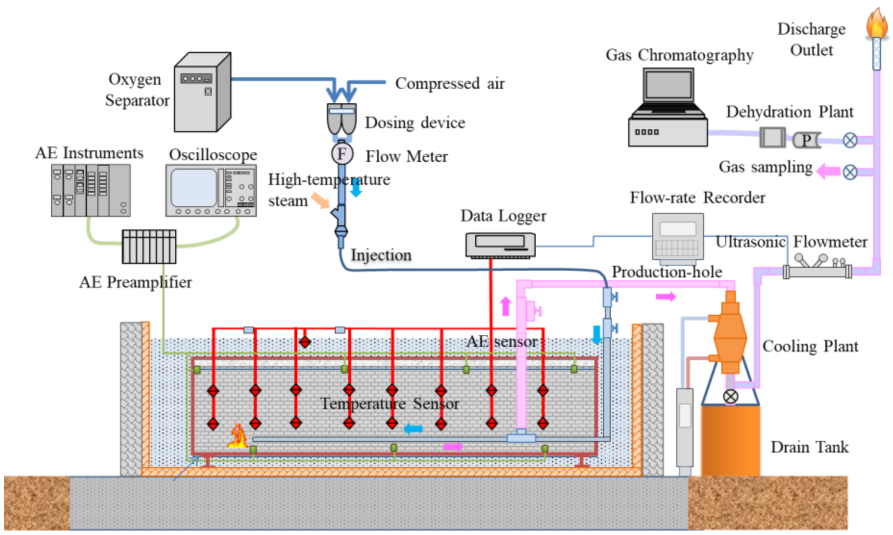

Fig. 1. UCG simulation experiment system

2.2 Coal sample

During the heating process of the coal sample in which the coal seam is gasified and burned along the bedding plane, the gasification zone is more likely to expand. Therefore, when constructing a horizontal coaxial UCG model gasifier, the gasification channel is set parallel to the bedding plane of the coal sample. In the experiment, a coal seam of 2700 × 550 × 600 mm (length × width × height) was constructed by combining coal samples with a length and width greater than 600 mm, as shown in Fig. 2(a). Cement and pulverized coal (1:10 ratio) filled the gaps between the coals, as shown in Fig. 2(b). The outer wall of the coal seam is covered with refractory cement to prevent heat release and gas leakage, as shown in Fig. 2(c). Table 1 shows the proximate and ultimate analysis of coal samples.

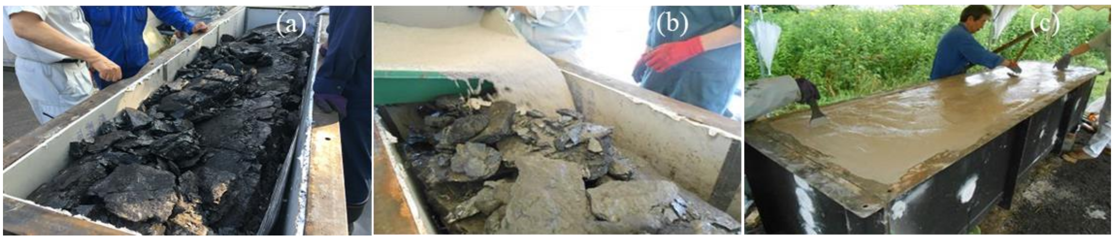

Fig. 2. Construction of UCG model

Table 1. Proximate analysis and ultimate analysis of coal samples

Calorific value (MJ/kg)	Proximate analysis (wt%)				Ultimate analysis (wt%)				
	Moisture	Ash	Volatiles	Fixed carbon	C	H	N	S	O
32.12	2.10	4.30	43.10	50.50	78.40	5.74	1.44	0.07	9.94

2.3 Arrangement of gasification channels

The vertical section of the experimental simulation system is shown in Fig. 3. A horizontal coaxial gasification passage 45 mm in diameter and 2600 mm in length was drilled with a 45 mm diameter auger at a height of 100 mm from the bottom of the steel vessel. Taking pictures of the inside of the gasification channel with an endoscope, it can be seen that coal exists around the gasification channel of each section, and the hole wall is kept in good condition and does not collapse, as shown in Fig. 4.

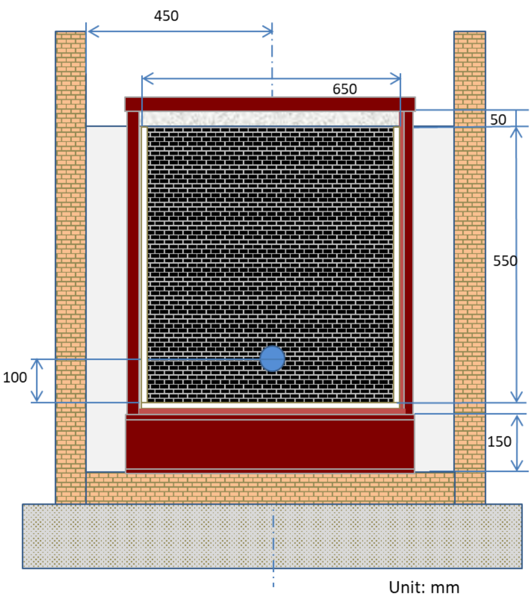

Fig. 3. Vertical section view of the gasifier

2500 mm from drilling 1600 mm from drilling 700 mm from drilling

Fig. 4. Inside the gasification channel

The main gasifier in the experimental system is installed in a steel container, and the gasification channel is a horizontal coaxial type. An injection pipe is inserted from the drill hole, and a mixed gas (gasification agent) of oxygen and air can be injected from the inside of the injection pipe. By continuously injecting a certain amount of gasification agent, combustion and gasification can be carried out inside the coal seam. The generated gas is guided from the outside of the injection pipe and the hole wall to the production pipe connected to the nozzle for later analysis and processing. To analyze the spatial distribution of temperature, acoustic emission and combustion cavity over time during the gasification process, a two-dimensional coordinate system was established with the bottom of the gasification channel as the origin, as shown in Fig. 5.

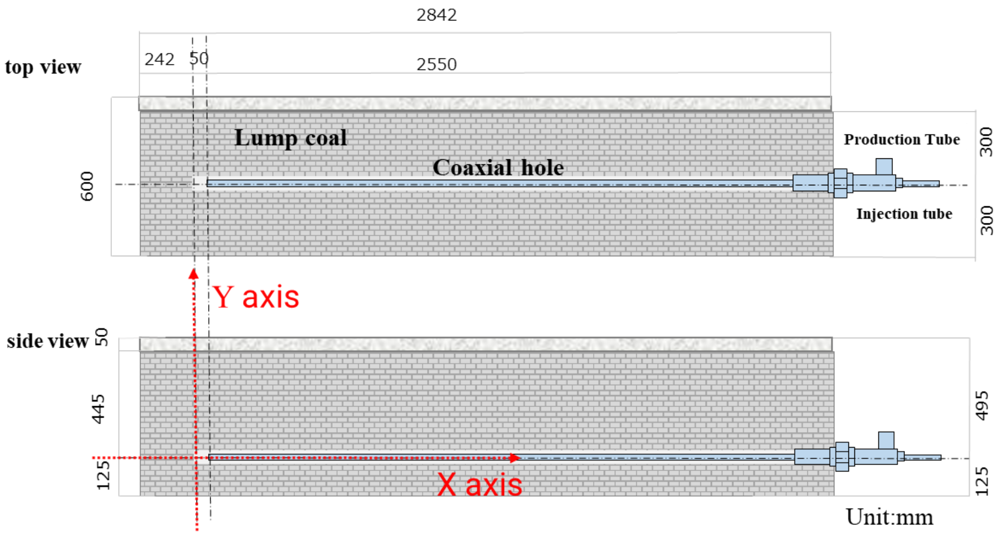

Fig. 5. Horizontal coaxial gasification channel

2.4 Sensor arrangement

2.4.1 Temperature sensor

Fig. 6 shows a schematic diagram of the buried position of each temperature sensor. Starting from the position 50 mm away from the bottom of the gasification channel, temperature sensors T1-1~T1-8 are placed directly above the gasification channel, temperature sensors T2-1~T2-8 are placed 150 mm above the gasification channel, and temperature sensors T3-1~T3-8 are placed 300 mm above the gasification channel. The horizontal interval between adjacent sensors is 300 mm. T4-1~T4-4 are embedded in 100 mm of the negative half-axis of the X-axis, with a height interval of 100 mm. Temperature sensors T4-1 to T4-1 are used to observe the temperature distribution at different heights. Fig. 7 shows the temperature sensor embedded on the top and side of the steel container.

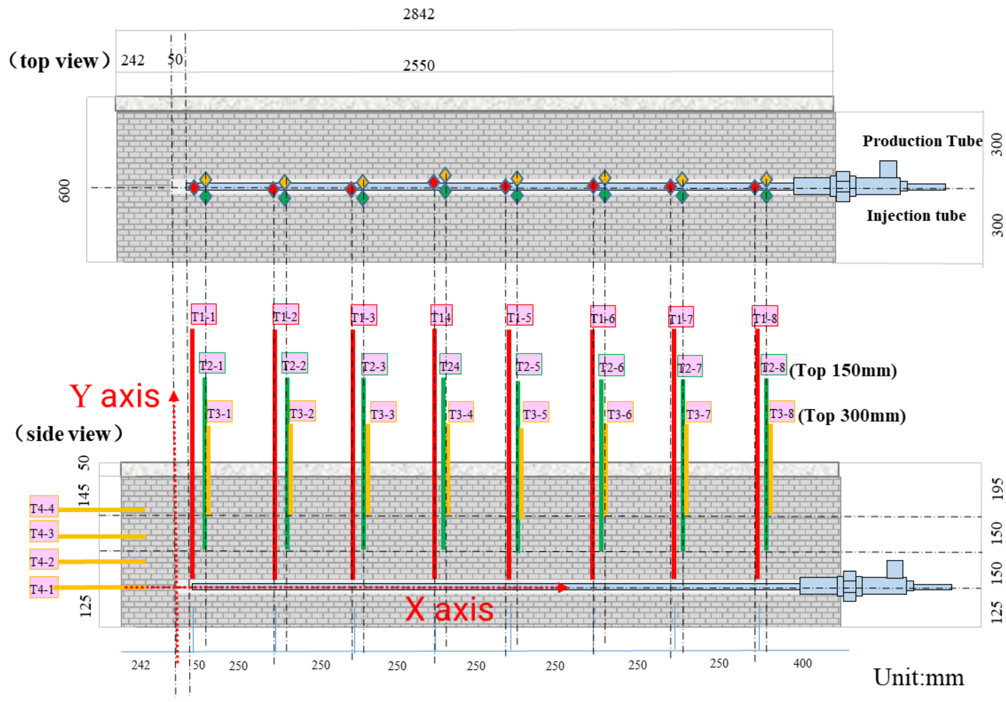

Fig. 6. Layout of temperature sensors

Fig. 7. The temperature sensor buried above and to the sides of the steel container

2.4.2 Acoustic emission (AE) sensor

During the UCG process, the high temperature causes thermal stress inside the coal seam, and microcracks occur. Acoustic emission signals are generated in the gasification process, and the faster the temperature change of the coal sample is, the more active the acoustic emission activity is [25]. To monitor the expansion of the surrounding damage area during the combustion process, acoustic emission sensors that detect minor damage were arranged around the lump coal sample.

In this experiment, all acoustic emission sensors are installed on the side of the steel container shell of the gasifier. Multiple 8 mm diameter holes were drilled from the steel vessel shell, the waveguide rod was inserted and the end of the waveguide rod was ensured to enter the coal seam. The gap was filled, the waveguide rod was fixed with refractory glue, and the gap between the coal and the steel vessel shell was filled with heat-resistant cement. After the cement is cured, the acoustic emission sensor is mounted on the waveguide rod. Fig. 8 is a schematic diagram of the configuration of the acoustic emission sensor. Fig. 9 shows the setting method of the acoustic emission sensor. Fig. 10 is a schematic diagram of the installation of the acoustic emission sensor on the sidewall of the steel container.

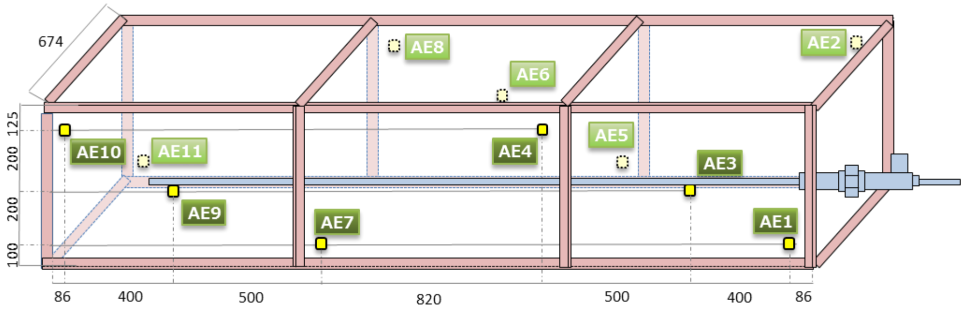

Fig. 8. Configuration diagram of the acoustic emission sensor

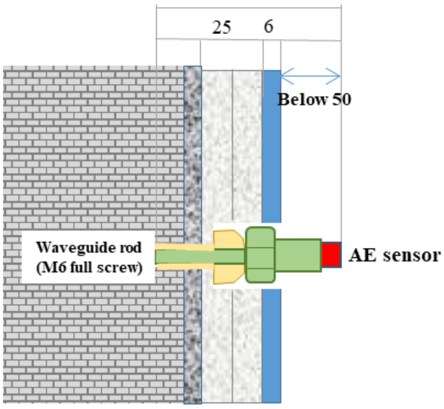

Fig. 9. Setting method of the acoustic emission sensor

Fig. 10. Acoustic emission sensor set on the sidewall of the steel container

2.5 UCG experimental process

In this experiment, the gasification combustion area was changed by moving the position of the injection pipe port. At the beginning of the experiment, the injection pipe port was located 350 mm from the bottom of the gasification channel, that is, Point (350,0). After 24 h, 38 h, 47 h, and 63 h of ignition, the port of the injection pipe was moved several times by 300 mm to the positive half-axis direction of X. Fig. 11 depicts the oxygen injection flow rate and total injection volume per minute during the experiment. The total flow rate of 0~24 h of injection was set to 30 L/min, of which oxygen was 15 L/min, and the total flow rate of 24~73 h was increased to 40 L/min, of which oxygen was 20 L/min. After 73 h, nitrogen and carbon dioxide were injected into the gasifier to extinguish the fire. The experimental process was divided into six stages according to the injection pipe port and the gasification agent flow rate. Moreover, the time points were 0~24 h, 24~38 h, 38~47 h, 47~63 h, 63~73 h, and 73~83 h.

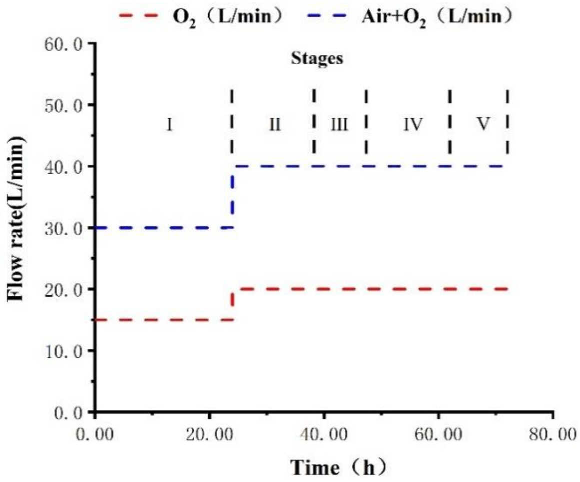

Fig. 11. Oxygen injection amount and total injection amount in the experiment

The pressure was recorded after successful ignition, which produced a large amount of flammable gas. The pressure was recorded after successful ignition, which produced a large amount of flammable gas. During the experiment, the internal pressure of the cavity was in a positive state, fluctuating in the range of 0.06~0.10MPa, as shown in Fig. 12. Therefore, the interior of the cavity is in a stable state, which provides reliability for subsequent experimental data analysis. There was no evident gas leakage during the experiment, indicating that the refractory cement and cement have good sealing performance.

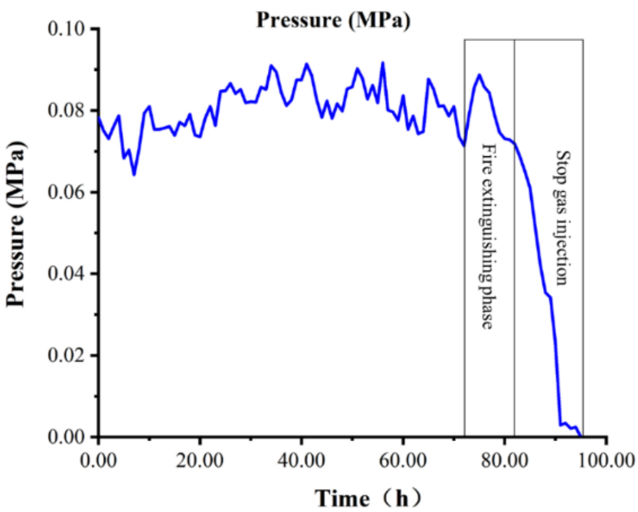

Fig. 12. Pressure changes during the experiment

3 Experimental results

3.1 Temperature change during gasification

Fig. 13 shows the temperature changes of temperature sensors T1-1 to T1-8, T2-1 to T2-8, T3-1 to T3-8, and T4-1 to T4-4 during the experiment. The coordinates of the injection pipe port at each stage of the experiment are shown in Table 2. The coordinate calibration of the temperature sensor is shown in Table 3.

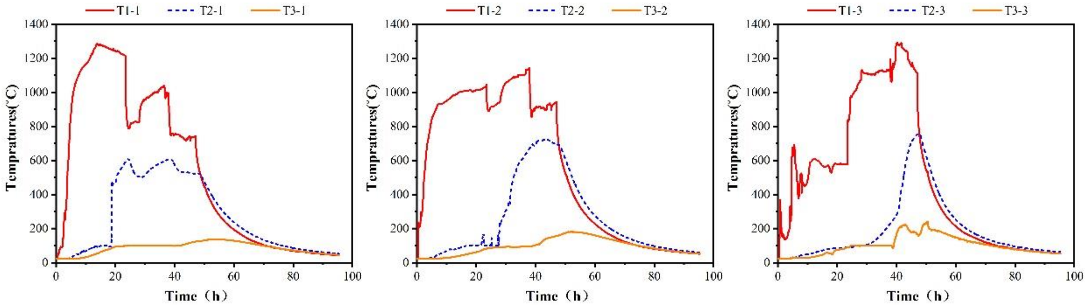

(a) T1-1~T1-3, T2-1~T2-3 and T3-1~T3-3

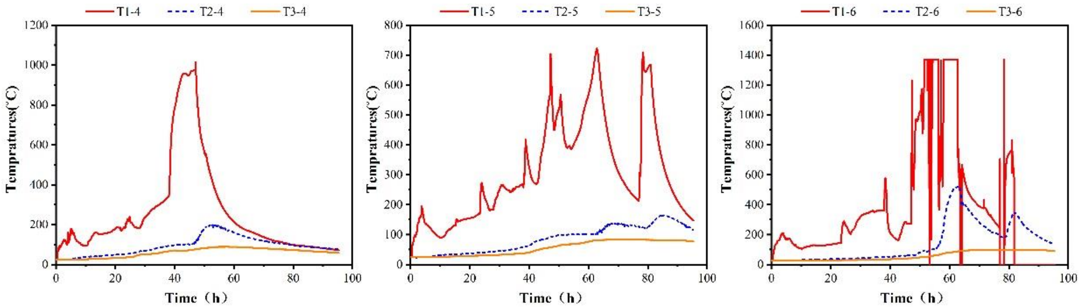

(b) T1-4~T1-6, T2-4~T2-6 and T3-4~T3-6

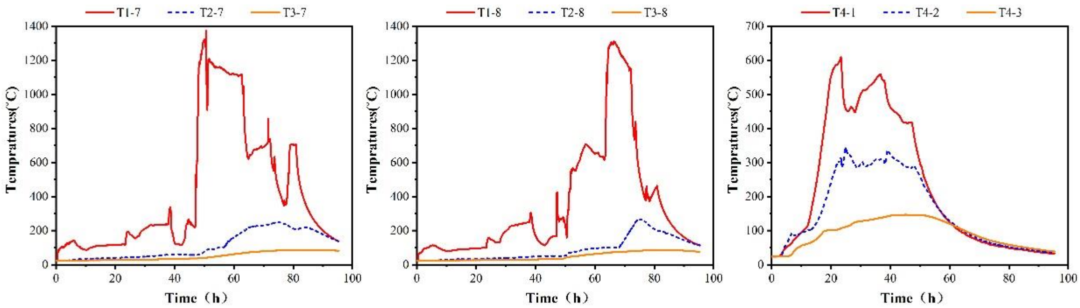

(c) T1-7~T1-8, T2-7~T2-8, T3-7~T3-8 and T4-1~T4-3

Fig. 13. Variation in temperature in the coal sample with time

Table 2. Coordinate calibration of the injection pipe port at each stage of the experiment (taking the bottom of the gasification channel as the coordinate origin)

Time(h)	0~24	24~38	38~47	47~63	63~73	73~83
Stage	Ⅰ	Ⅱ	Ⅲ	Ⅳ	Ⅴ	Ⅵ
Coordinates	350,0	650,0	950,0	1250,0	1550,0	1550,0

Table 3. Coordinate calibration of the temperature sensor (taking the bottom of the gasification channel as the coordinate origin)

	1	2	3	4	5	6	7	8
T1~	50,0	350,0	650,0	950,0	1250,0	1550,0	1850,0	2150,0
T2~	50,150	350,150	650,150	950,150	1250,150	1550,150	1850,150	2150,150
T3~	50,300	350,300	650,300	950,300	1250,300	1550,300	1850,300	2150,300
T4~	-100,0	-100,100	-100,200	-100,300				

The port of the injection pipe starts to ignite at X=350 mm, and after 24 h, 38 h, 47 h, and 63 h, the port of the injection pipe moves to the positive half-axis of X at a scale of 300 mm.

The temperature sensors T1-1~T1-8 are arranged at the same level as the gasification channel. The temperatures of T1-1 and T1-2 sharply rose after ignition. The temperature of T1-3 sharply increased after 24 h and reached a local temperature peak at 28 h. As the experiment progressed, the high-temperature area moved to the positive semiaxis of the x-axis. After 38 h, the temperature of T1-4 sharply rose, reaching a local peak at 42 h. After 47 h, the temperatures of T1-5, T1-6, and T1-7 sharply increased. The temperature of T1-5~T1-7 reached a local peak at 51 h. The temperature of T1-8 sharply rose after 63 h and reached a local peak at 67 h. The change in the position of the injection pipe port was the same as the time node when the temperature of T1-1~T1-8 began to rise. With the injection pipe's movement, the gasification agent's supply area changed, and the gasification area moved accordingly. Therefore, by moving the position of the injection pipe port, the combustion gasification reaction of the unreacted coal region can be promoted, and the gasification region can be guided to expand in a predetermined direction. In addition, the flow rate and composition of the gasification agent injected within 24~73 h were the same. The coal violently burned within approximately four hours after the injection pipe was moved, and the temperature rose faster. The local temperature peaked at four hours, indicating that after the continuous injection of the gasification agent for four hours, the combustion was the most intense.

The maximum temperature of temperature sensors T1-4 and T1-5 in the middle of the gasification channel is approximately 800°C, while the maximum temperature of T1-1~T1-3 and T1-6~T1-8 at both ends exceeds 1000°C. Therefore, the scale of coal combustion is smaller in the area containing temperature sensors T1-4 and T1-5 than in the other areas. Temperature sensors T2-1 to T2-8 are embedded with the coordinate axis Y= 150 mm. The maximum temperature of T2-4 to T2-5 in the middle of the gasification passage is below 300°C, but the maximum temperature of T2-1 to T2-3 and T2-6 on both sides reaches 600°C to 800°C. This phenomenon shows that the degree of gasification is small between X=950~1250 mm in the middle of the gasification channel, and the upper boundary of the central coalbed gasification area is not developed to 150 mm above.

Temperature sensors T3-1 ~ T3-8 are buried at the coordinate axis Y = 300 mm, and the overall maximum temperature is below 200°C. There is no combustion in the entire area at this height, so the upper boundary of the artificial coalbed gasification area is located on the coordinate axis Y = in the range of 150 mm to 300 mm.

The temperature sensor T4-1 is buried at coordinate axis X= -100 mm, and its maximum temperature exceeds 600°C; T4-2 is buried at 100 mm above T4-1, and its maximum temperature exceeds 300°C. Thus, the left boundary of the gasification area is located at coordinate axis X= -100 mm.

3.2 Correlation analysis between high-temperature regions and acoustic emissions

For convenience, X=-150~950 mm is the left side of the artificial coal seam, X=950~1250 mm is the middle of the artificial coal seam, and X=1250~2350 mm is the right side of the artificial coal seam. The temperature data were analyzed and processed in combination with the position of the temperature sensor, and the expansion process of the high-temperature region of the gasification zone during the experiment was obtained, as shown in Fig. 14.

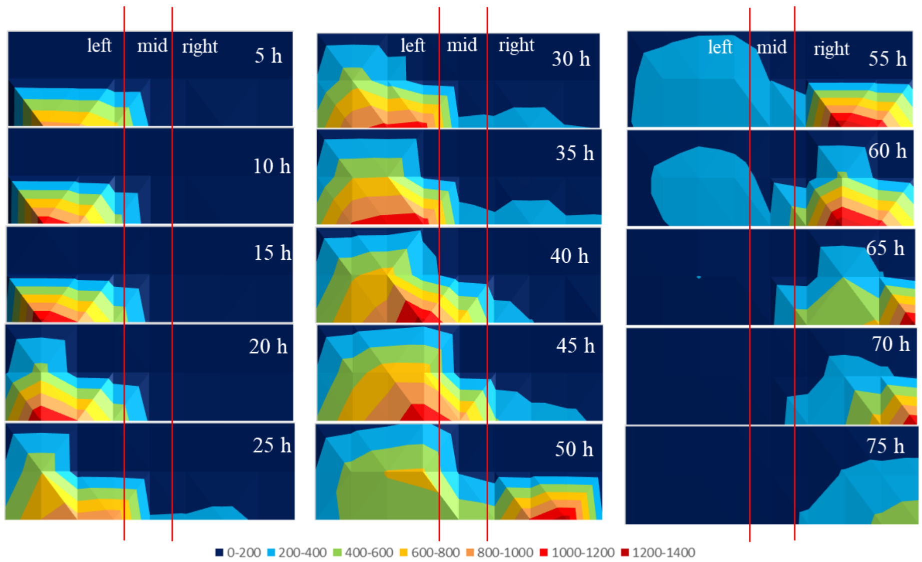

Fig. 14. High-temperature area expansion diagram

From 0~24 h, the temperature on the left side of the coal seam rapidly increased after ignition was successful. From 24~38 h, the overall temperature gradually increased, developed from the left side of the coal seam, gradually expanded to the middle of the coal seam, and finally reached the highest temperature on the left side. This shows that the gasification region of 0~38 h is on the left side of the coal seam. From 38~63 h, the temperature in the central area gradually increased, and the temperature in the left area gradually decreased. The high-temperature field migrated to the right side across the middle of the coal seam and finally reached the highest temperature on the right side. This shows that the 38~63 h gasification area is on the right side of the artificial coal seam. From 63~73 h, the temperature of the gasification area on the right side gradually decreased, and the high-temperature field migrated to the right boundary of the coal seam. In short, the distribution range of high-temperature areas on the left side of the coal seam is more extensive than that on the right side, and the low-temperature areas are concentrated in the middle and upper parts of the coal seam.

The calibration results of the AE source and the distribution results of the highest temperature in the coal seam at the five stages are shown in Fig. 15. In the distribution diagram of the AE source calibration results, different colors represent the acoustic emission events generated in different stages, the position of the ball indicates the location of the acoustic emission, and its size indicates the relative energy, that is, the size of the damage scale.

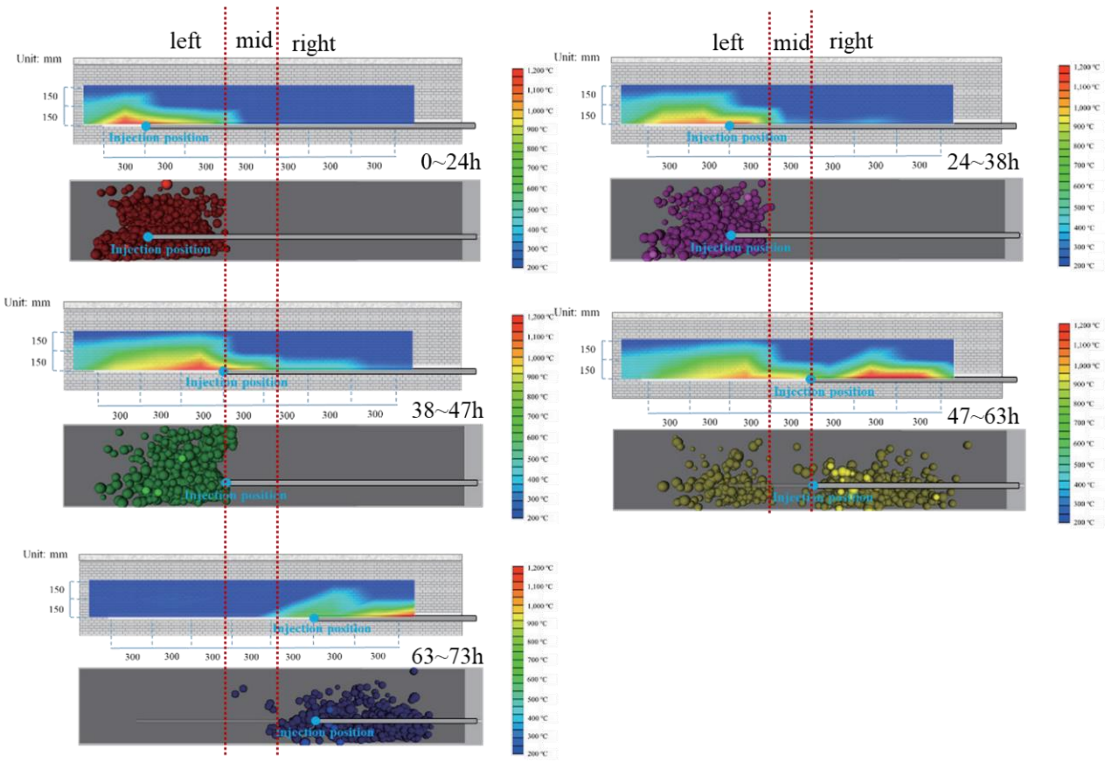

Fig. 15. AE source calibration results and maximum temperature distribution in the coal seam (side view)

From 0~47 h (Ⅰ~Ⅲ), many AE events were generated from the bottom to the top of the coal seam. However, within 47~73 h (Ⅳ~Ⅴ), many AE events occurred from the bottom to the middle of the coal seam, and fewer occurred above. This trend is consistent with the fact that the high-temperature area of the temperature profile extends in the upper part of the left side, while the high-temperature area is lower on the right side.

Within 0~47 h (Ⅰ~Ⅲ), on the left side of the coal seam, the high-temperature area expands over a wide range, and the AE source is also widely distributed.

Within 47~63 h (Ⅳ~ Ⅴ), on the left side of the coal seam, the distribution of high-temperature areas is small, and the distribution of AE hypocenters is also scattered. The temperature rise in the middle of the coal seam is tiny, and the AE source is hardly calibrated. On the right side of the coal seam, the high-temperature region is enlarged relative to the left side, and the AE source is widely distributed relative to the left side.

Throughout the experiment, the position of the AE shifted with the movement of the high-temperature region. From 0~73 h, the high-temperature area gradually moved to the right side of the coal seam, and the AE source calibration results also showed the same moving trend.

3.3. Gasification zone and combustion cavity growth process

3.3.1 Profile of the gasified coal sample

After the experiment, consisting of several hours of nitrogen and carbon dioxide to extinguish the fire, three vertical holes were drilled from the artificial coal seam to the gasification channel. The gypsum solution was poured into the lump coal sample. After the gypsum solidified, the block coal sample was cut to observe the condition of the vertical section. The artificial coal seam was cut at intervals of 100 mm, and the expansion of the gasification area on the vertical section was observed. Fig. 16 shows the positions of each section (Sections 5, 14, and 23 are the drilling positions). The coordinates of the sections are shown in Table 4.

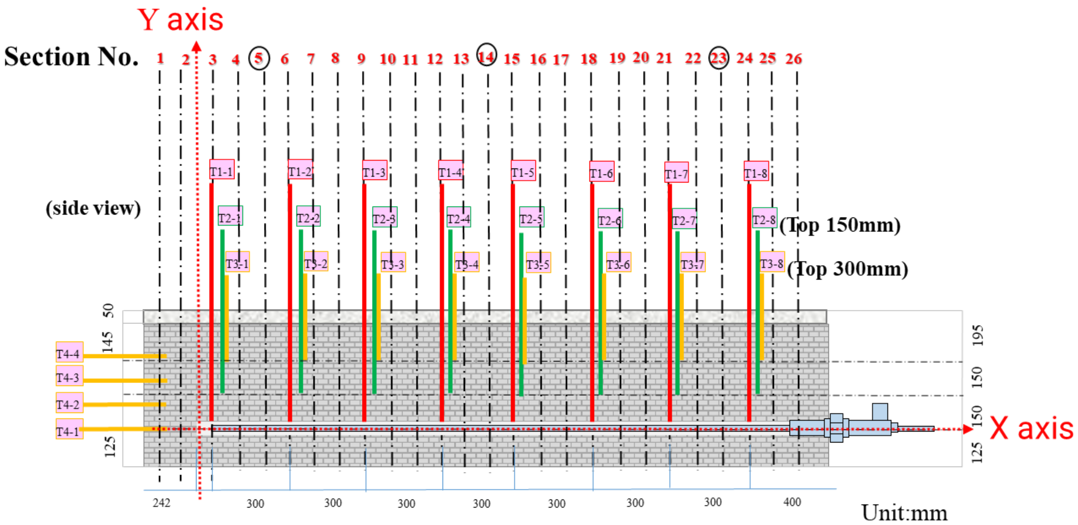

Fig. 16. Profile location, profile number and configuration of the temperature sensor (side view)

Table 4. Coordinate calibration of the section (taking the bottom of the gasification channel as the coordinate origin)

No.	1	2	3	4	5	6	7	8	9	10	11	12	13
X=	-150	-50	50	150	250	350	450	550	650	750	850	950	1050
No.	14	15	16	17	18	19	20	21	22	23	24	25	26
X=	1150	1250	1350	1450	1550	1650	1750	1850	1950	2050	2150	2250	2350

After grouting the cavity formed by the artificial coal seam gasification process, the cut section is shown in Fig. 17. The figure marked T1-1~T1-8 is the section of the buried temperature sensor. In Profiles No. 5, No. 14, and No. 23, the vertically extending white portion is the trace of drilling when gypsum was injected. Sampling and analysis of the residues in the section is performed, similar components are classified into the same area, and each section is roughly divided into the combustion cavity, the gasification area, the unreacted coal area and the cement-filled area, as shown in Fig. 18.

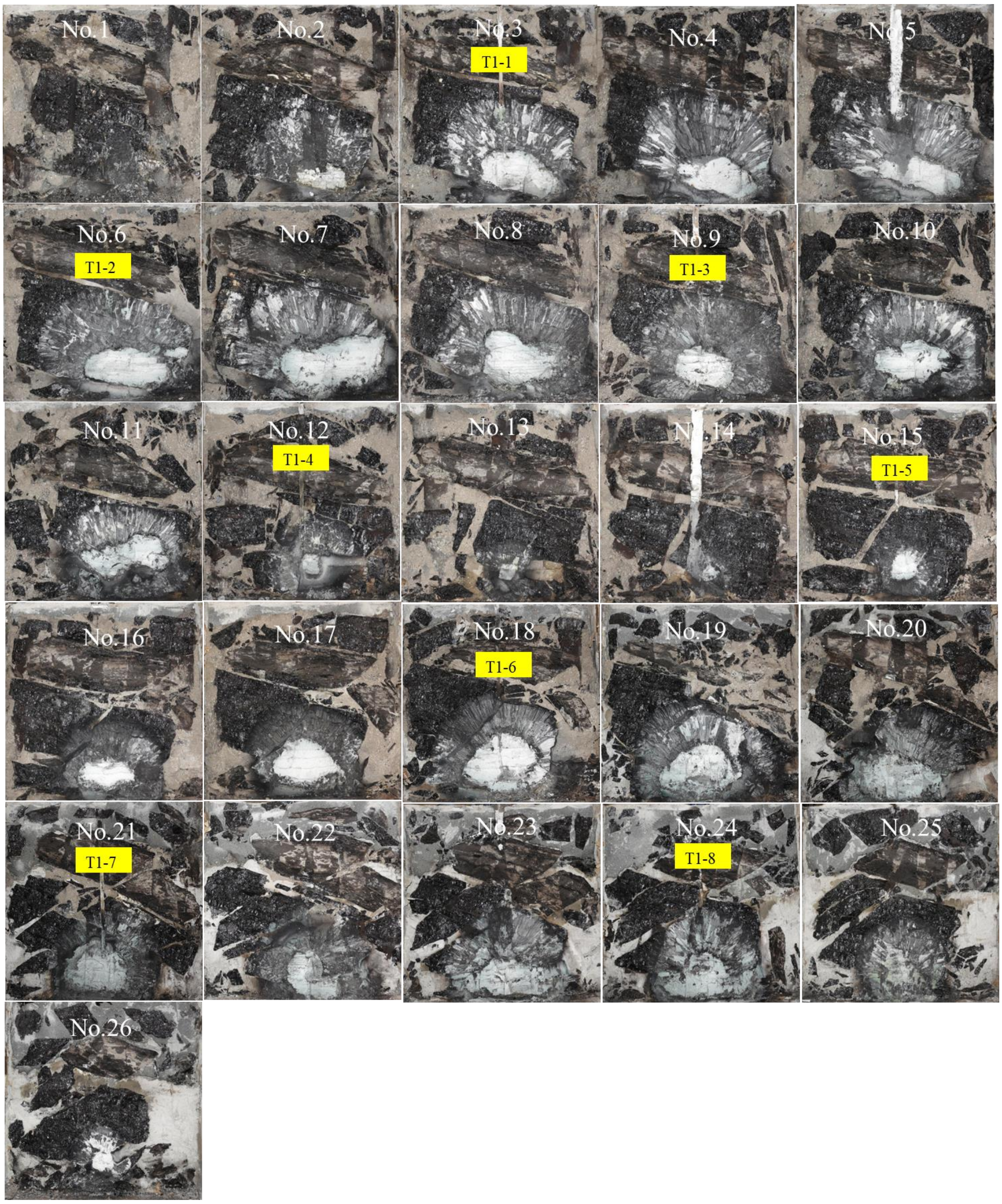

Fig. 17. Profiles after grouting the cavity formed by the artificial coal seam gasification process

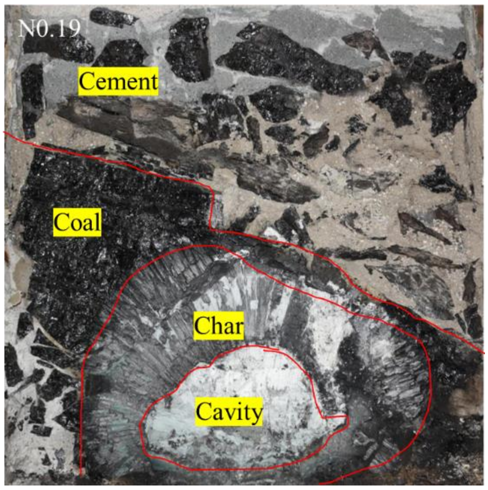

Fig. 18. Distribution of different regions

According to the temperature of the coal seam, chemical reaction and product gas composition, the underground gasification process is divided into an oxidation zone, reduction zone and dry distillation zone along the gasification channel [30], as shown in Fig. 19. In the oxidation zone, carbon combustion mainly occurs, releasing much heat, and the temperature is above 900°C. Adjacent to the oxidation zone is the reduction zone. The gas flow generated in the oxidation zone reaches the reduction zone along the gasification channel, the heat generated makes the coal seam in the reduction zone in a hot state, and the temperature is between 550 and 900°C. The dry distillation zone follows the reduction zone. The oxygen-free high-temperature gas flow produces pyrolysis on the coal in the dry distillation zone to promote water analysis and volatilization in the coal. The temperature is between 200 and 550°C. After a series of reactions in the three reaction zones, mixed gas with combustible components, mainly H_2, CH_4 and CO, was generated. With the continuous combustion of the coal seam, the three reaction zones gradually move to the production pipe, and the gasification zone continuously advances in the forward radial and axial directions, thus maintaining the continuous gasification reaction process.

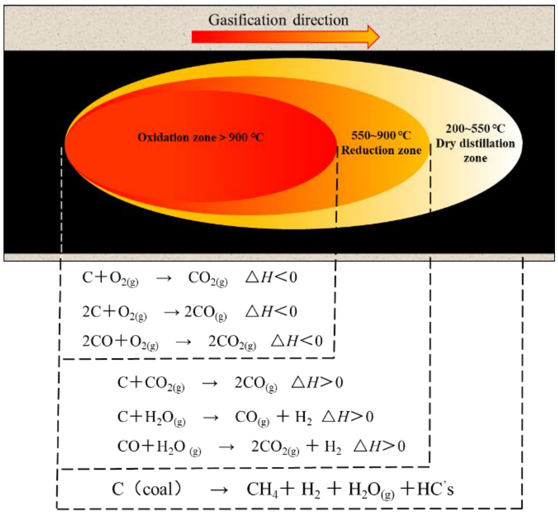

Fig. 19. Schematic diagram of the underground coal gasification reaction process

Due to the different gasification temperatures and the main reactions that occur, the composition of the residues in the three regions must be different. The residue in the oxidation zone is mainly ash, the residue in the reduction zone is mainly gasification residual char, and the residue in the dry distillation zone is mainly pyrolysis semichar [31-32]. Combined with the distribution law of the temperature field in the simulated gasification process, the residues in the three regions were collected along the direction of the gasification channel. The proximate and ultimate analyses of the residue samples are shown in Table 5. Comparing these results with the corresponding initial coals, the ash residue in the oxidation zone contains a small amount of unburned carbon. The char residue in the reduction zone has a lower volatile and slightly higher fixed carbon content than the pyrolysis semichar in the dry distillation zone. This is because the coal seam first goes through drying and retorting, and then gasification occurs at a higher temperature, resulting in a lower volatile content of residual char in the reduction zone and a higher fixed carbon content [33]. In the initial coal of this experiment, element C mainly migrated to the gasification of pure carbon, element H mainly migrated to CH_4 and H_2, element O mainly migrated to CO, CO_2 and residues, and element S and element N mainly migrated to residues.

Table 5. Proximate and ultimate analysis of three zone residuals

	Proximate analysis (wt%)			Ultimate analysis (wt%)				
	Ash	Volatiles	Fixed carbon	C	H	N	S	O
Initial coal	4.30	43.10	50.50	78.40	5.74	1.44	0.07	9.94
Oxidation zone	85.64	78.69	23.65	—	—	—	—	—
Reduction zone	9.65	3.61	97.57	90.47	0.23	0.82	0.08	3.98
Dry distillation zone	7.27	5.86	95.68	90.19	0.34	1.73	0.07	2.54

3.3.2 2D reconstruction of the gasification zone and combustion cavity

(1) Identification of the gasification zone and combustion cavity

A side view was made with gasification channels by using cross-sectional modeling. The combustion cavity, gasification area, unreacted coal area, and cement-filled area are distinguished by color, as shown in Fig. 20 and Fig. 21. In these figures, the white represents the combustion cavity, the gray represents the gasification area, the black represents the unreacted coal area, and the vermilion represents injected cement area. The two-dimensional gasification and combustion cavity constructed according to the distribution map is shown in Fig. 22.

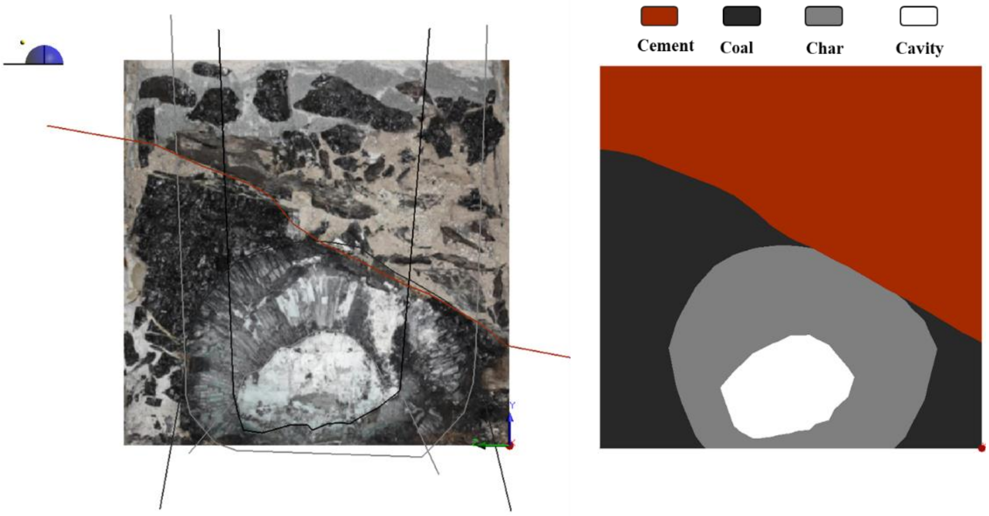

Fig. 20. Side view made by cross-sectional modeling

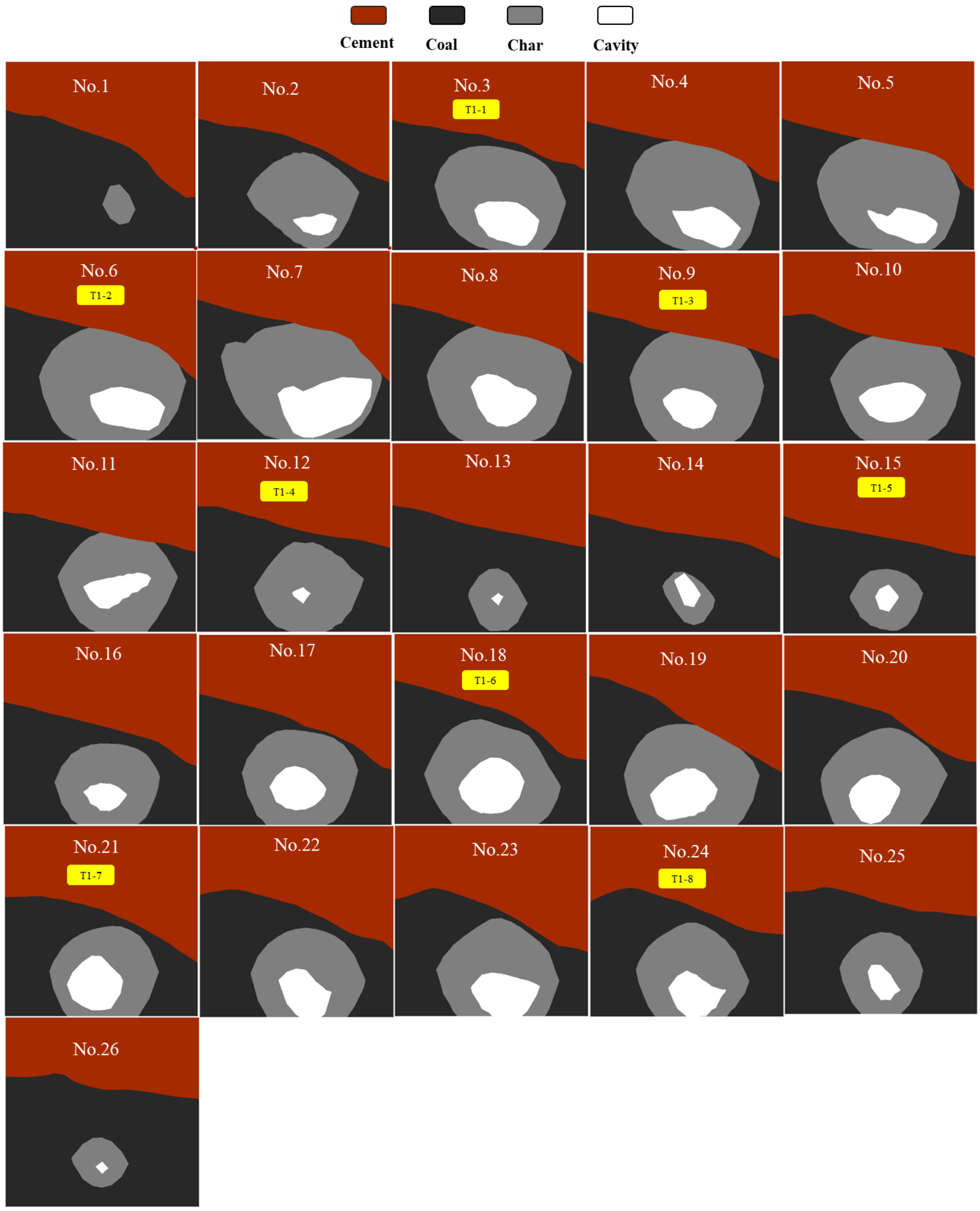

Fig. 21. Profile side view

The section on the left side of the ignition position (the ignition position is X=350 mm) is within -150 mm to -50 mm from the coordinate origin. After ignition is successful, the coal burns to the left and gradually gasifies, and the combustion cavity and gasification area gradually decrease as the distance from the ignition point increases, as shown in Profiles 1 and 2 in Fig. 21.

Within 50 mm to 850 mm from the coordinate origin, the expansion trend of the combustion cavity and the gasification area is stable, and the distribution range is the largest, as shown in Profiles 3 to 11 in Fig. 21. In this range, the maximum temperature inside the gasification channel is 1200-

1500°C, the maximum temperature at 150 mm above the gasification channel is 600-750°C, and the temperature at 300 mm is below 200°C, indicating that the boundary of the gasification region is in the range of Y=150 mm~300 mm. The upper boundary of the gasification zone did not reach Y=300 mm due to the influence of the cement filling layer and rock layer, and the gasification zone may be further expanded if larger coal blocks are present.

Within 950 mm to 1250 mm from the coordinate origin, the expansion range of the combustion cavity and the gasification area is the smallest, as shown in Profiles 12 and 15 in Fig. 21. Profiles 12 to 15 are in the middle of the artificial coal seam. The temperature rise trend in the middle of the high-temperature derivative map of the gasification zone is minimal compared to that of the two sides. The AE source is almost not calibrated and interrupted in the middle. Profile 14 shows that there are many filled cement layers around the gasification channel, and the coal is divided, which restricts the expansion of the gasification area to the outside. There are cement filling layers on the left and right sides and above Profile 15. The maximum temperature of 150 mm above the gasification channel of this profile is approximately 800°C, which is lower than that of the 50 mm~850 mm profile over 1200~1500°C. The presence of cement around profile 15 limits coal combustion.

Within 1350 mm to 1550 mm from the coordinate origin, the expansion range of the combustion cavity and the gasification area gradually increases, as shown in Profiles 16 and 18 in Fig. 21. In the high-temperature derivative map of the gasification zone, the mid-temperate zone is concentrated in this area, and the AE source calibration gradually increases. The maximum temperature 150 mm above the gasification channel is approximately 520°C, indicating that the gasification region extends to the range of Y=150 mm~300 mm but does not reach Y=300 mm. In addition, in the X=1550 mm section, there is a cement filling layer approximately 10 mm wide in the upper left. However, the gasification area extends beyond this cement filling layer into the adjacent coal block.

Within 1650 mm to 2150 mm from the coordinate origin, the expansion trend of the combustion cavity and the gasification area is stable, as shown in Profiles 19 and 24 in Fig. 21. In the high-temperature derivative map of the gasification zone, the high-temperature zone is distributed in this range, and the AE source calibration distribution is concentrated.

Within 2250 mm to 2350 mm from the coordinate origin, the expansion trend of the combustion cavity and the gasification area gradually decreases, as shown in Profiles 25 and 26 in Fig. 21.

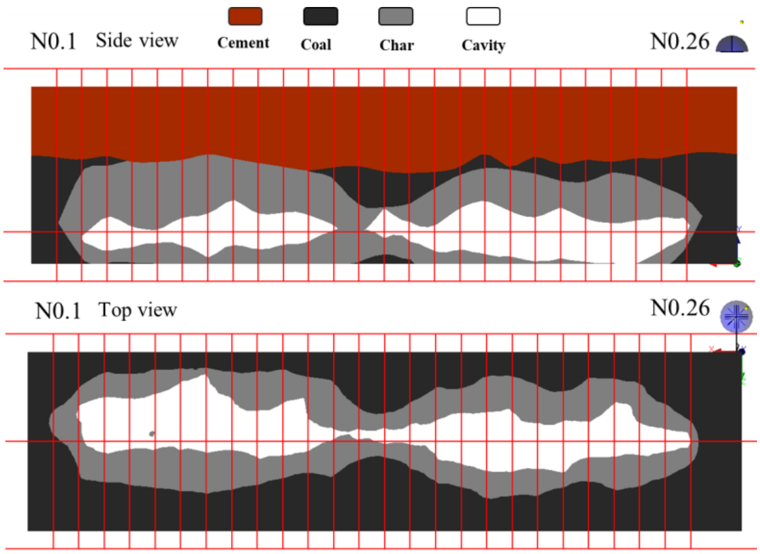

Fig. 22. Two-dimensional gasification and combustion cavity constructed from a cross-sectional distribution map (side and top views)

(2) Relationship between the combustion cavity and the temperature and acoustic emission

Fig. 23 shows the comparison of the two-dimensional section of the combustion cavity, the temperature distribution, and the calibration results of the AE source. First, in the left and suitable regions where the high-temperature region is widely distributed, the AE source distribution range is extensive, and the combustion cavity and gasification region, which are relatively developed in the middle, are fully expanded. The light blue to green (400-600°C) mid-temperature area is widely distributed on the left side. In addition, the AE activity in the left area is more intense. The cutting section shows that the combustion area has expanded to the left boundary of the coal seam. The AE source calibration results and temperature distribution in the coal seam are consistent with the constructed two-dimensional combustion cavity. Second, the temperature rise near the middle of the coal seam is tiny, the high-temperature area is smaller than the range on both sides, and AE events are rarely generated.

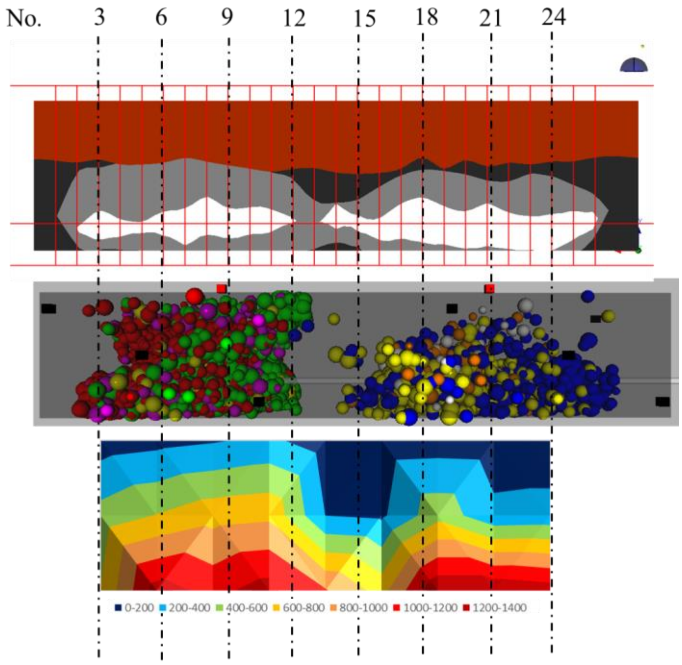

Fig. 23. Comparison of the combustion cavity and the temperature distribution of the section reconstruction and the calibration results of the AE source

3.3.3 Analysis of combustion cavity shape

In the process of UCG, when the temperature is higher than 400℃, the coal seam will react and form the corresponding gasification area, and when the temperature is higher than 800℃, the combustion cavity will be formed. The region where the two-dimensional temperature cloud map in Fig. 24 is higher than 800°C is the combustion cavity, and its shape is consistent with the shape of the cross-sectional reconstruction of the two-dimensional combustion cavity. Therefore, the temperature change in the gasifier can effectively and intuitively reflect the gasification process. The high-temperature area in the gasifier corresponds to the more intense area in the gasification reaction, reflecting the growth process of the combustion cavity.

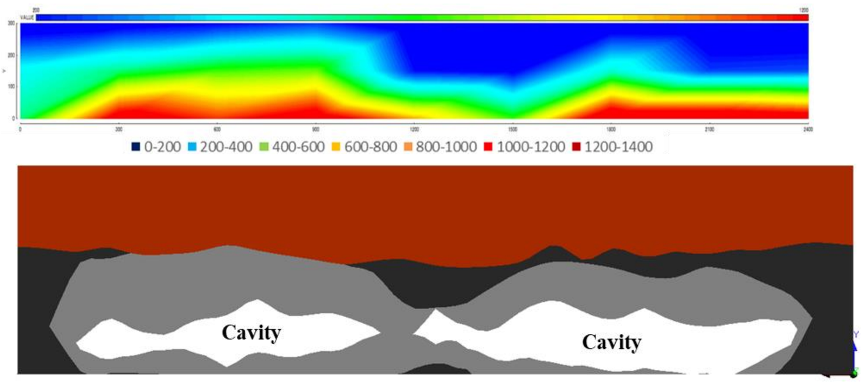

Fig. 24. Combustion cavity shape

3.4 3D construction of the gasification region and combustion cavity

Using the two-dimensional cross-sectional data of the 26 gasification zones and combustion cavities in Fig. 21, the three-dimensional shapes of the combustion cavity and the gasification zone are constructed, as shown in Fig. 25. In the horizontal coaxial UCG system, the gasification region is cylindrical with the gasification channel as the axis, and the radius of the cylinder increases with the increase in the degree of gasification. The cylinder on the left has an enormous volume, indicating the most violent degree of gasification. The cement filling layer around the middle of the gasification channel limits coal combustion, so the gasification area and combustion cavity are minimal. The gasification area on the right has a cement layer as an interlayer, which restricts the upward combustion of coal. Thus, the gasification area and combustion cavity are slightly smaller than those on the left. The concentrated area of AE source calibration and the high-temperature area in the coal seam are consistent with the fully expanded area of the constructed three-dimensional combustion cavity. According to the overall volume estimation by grid division, the combustion cavity is 50.774 cm^3, the gasification area is 237.007 $cm^{3,}$ and the artificial coal seam is 485.669 cm^3. The total amount of coal that fully underwent gasification was 10.5%; the total amount of coal that did not complete gasification was 48.8%.

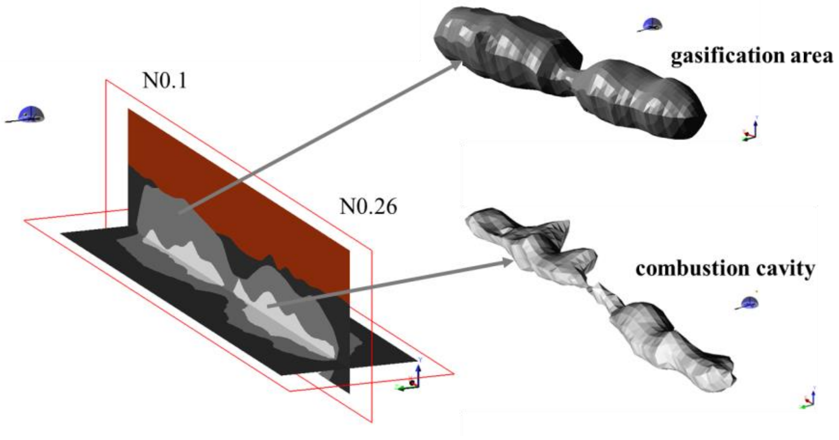

Fig. 25. 3D shapes of the combustion cavity and gasification zone

3.5 Product gas

Two methods were used to measure product airflow. One is to calculate the product gas flow through the nitrogen concentration. Assuming that all the nitrogen in the injected gasification agent is exhausted, the product gas flow is calculated according to the amount of injected nitrogen and the nitrogen concentration in the product gas analyzed by gas chromatography. The other measures the product gas flow during the experiment through an ultrasonic flowmeter. The comparison between the two is shown in Fig. 26. The ultrasonic flowmeter calculates the product gas flow according to the average movement of the gas. In contrast, once an hour, the nitrogen gas calculates the product gas flow according to the gas analysis's (instantaneous value) value. The two results show similar trends, indicating that the cavity's interior is stable, and the whole experiment has good airtightness.

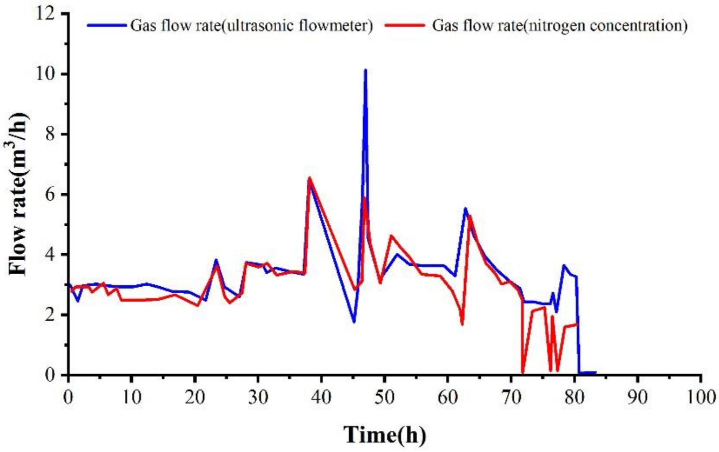

Fig. 26. Product gas flow

Fig. 27 shows the main components and calorific value of the product gas. The changing trend of the product gas composition is consistent with the monitoring results of the temperature sensor, and there are remarkable changes after the beginning of each stage. The combustible gases such as CO, H_2, and CH_4 increase sharply after the start of the test or after the port of the injection pipe is moved, and then gradually decrease. The calorific value of the product gas can be calculated according to the concentration of combustible gases such as H_2, CO, CH_4 and other hydrocarbons [30], and the change in the calorific value is the same as that of H_2, CO and CH_4. By moving the position of the injection tube port, the gasification area can be controlled to improve the calorific value of the product gas. When the quality of the product gas (flammable gas composition and calorific value) falls, the quality can achieve a sharp recovery by moving the filling pipe port, then gradually reducing the quality, and finally stabilized at 5MJ/Nm^3.

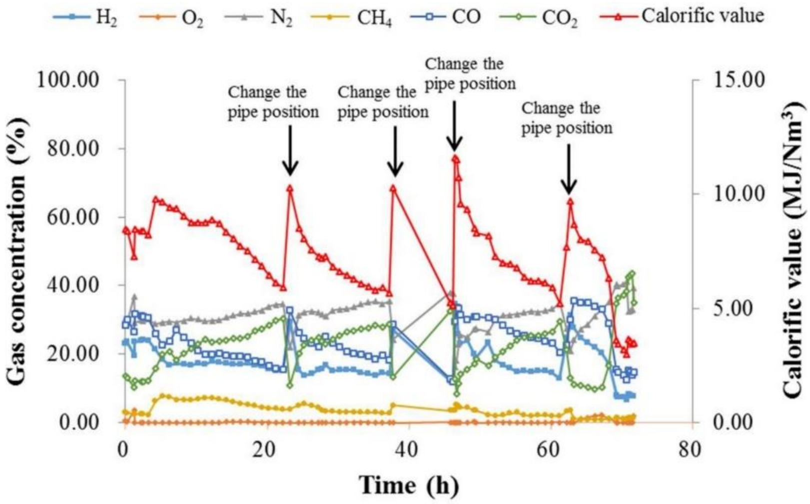

Fig. 27. Main compositions and the calorific value of product gas.

4 Conclusion

This paper used layered temperature monitoring and acoustic emission monitoring techniques to study the growth of the UCG combustion cavity in the horizontal coaxial gasification channel. After the experiment, the artificial coal seam was cut to obtain the section shape of the combustion cavity. Two-dimensional and three-dimensional gasification combustion cavities were constructed according to the profile shape, and were compared and verified with the monitoring results of temperature and acoustic emission. The main conclusions are summarized as follows:

In the gasification process of horizontal coaxial UCG, the nearby temperature rapidly rises with the movement of the injection pipe port, indicating that moving the injection pipe port can effectively guide the expansion direction of the gasification area. When the injection flow rate and composition of the gasification agent are the same, coal combustion is the most violent within four hours of the moving injection pipe. The local temperature exponentially increases, indicating that the combustion and gasification state is the most complete after four h of continuous ventilation.

The local temperature change is closely related to the AE activity in the gasifier. When the local temperature changes, the AE event gradually increases, and the movement of the AE source position is consistent with the movement of the high-temperature area. Combining the derivative movement in the high-temperature region and the AE source distribution, the combustion cavity's expansion process during the gasification process can be inferred. The calibration results of the AE source and the high-temperature derivation map in the horizontal coaxial UCG process are consistent with the 2D and 3D gasification combustion cavities reconstructed in the profile, indicating that AE and temperature monitoring can effectively infer the growth process of the gasification combustion cavity.

The horizontal coaxial UCG gasification zone is a cylinder with the channel as the axis, and the radius of the cylinder increases with the increase in the degree of gasification. This experiment has thick rock layers and cement interlayers in the middle of the gasification channel. Thus, the gasification area cannot be further expanded, indicating that the gasification process may be interrupted when large-scale gangue or collapsed columns appear in the coal seam during field production. In the profile X=1550 mm, a cement filling layer is approximately 10 mm wide in the upper left. However, the gasification area extends beyond this cement filling layer to the adjacent coal block, indicating that small-scale gangue has little influence on the gasification process.

Credit author statement

Fa-qiang Su: Investigation, Writing-Reviewing and Editing, Funding acquisition. Jun-bo Wu: Investigation, Writing-Original draft preparation, Funding acquisition. Tao-Zhang: Supervision, Validation. Qi-chao Deng: Investigation, Data curation. Akihiro Hamanaka: Conceptualization, Methodology. Yi-he Yu: Investigation, Validation, Data curation, Funding acquisition. Meng-jia Dai: Investigation, Validation. Jun-nan Yang: Validation, Resources. Xiao-long He: Investigation , Data curation.

Declaration of Competing Interest

The authors declare that they have no known competing financial interests or personal relationships that could have appeared to influence the work reported in this paper.

Acknowledgments

This work was supported by Key Laboratory of Western Mine Exploitation and Hazard Prevention, Ministry of Education (SKLCRKF1902), State Key Laboratory for Geomechanics and Deep Underground Engineering, China University of Mining & Technology (SKLGDUEK2004), Key R & D and promotion projects in Henan Province (222102320139), Henan Province Key Scientific Research Project Plan for Colleges and Universities (22B440003).

References

[1] Su Faqiang, Jing Shijie, Gao Xicai, Pu Hai, Fan Weitao, Yu Guanglei, Wu Junbo, Deng Qichao, Zhang Tao. Evaluation of combustion cavity development and energy recovery in underground coal gasification [J]. Coal Journal, 2021, 46(11): 3682-3691.

[2] Daggupati S,Mandapati R N,Mahajani R M ,et al. Laboratory studies on combustion cavity growth in lignite coal blocks in the context of underground coal gasification[J]. Energy, 2010, 35(6):2374-23867.

[3] Prabu V , Jayanti S . Simulation of cavity formation in underground coal gasification using bore hole combustion experiments[J]. Energy, 2011, 36(10):5854-5864.

[4] Wang F T , Mead S W , Stuermer D H . Groundwater contamination near the Hoe Creek UCG experiments. 1981.

[5] Wang F T , Mead S W , Stuermer D H . Mechanisms for groundwater contamination by UCG: preliminary conclusions from the Hoe Creek study. 1982.

[6] Raber E , Stone R . Ground-water hydrologic effects resulting from underground coal gasification experiments at the Hoe Creek Site near Gillette, Wyoming. Interim report, October 1979-March 1980. 1980.

[7] Mehdi, Najafi, Seyed, et al. Prediction of cavity growth rate during underground coal gasification using multiple regression analysis[J]. International Journal of Coal Science & Technology, 2015, 2(4):318-324.

[8] Nourozieh H , Kariznovi M , Chen Z , et al. Simulation Study of Underground Coal Gasification in Alberta Reservoirs: Geological Structure and Process Modeling[J]. Energy & Fuels, 2010, 24(MAY-JUN.):3540-3550.

[9] Pdf S . Modeling Cavity Growth in Underground Coal Gasification[J]. Journal of Energy, 2013, Vol. 7(no. 5):410-415.

[10] Chen, Liang~a, Hou, et al. A back analysis of the temperature field in the combustion volume space during underground coal gasification[J]. Mining Science and Technology, 2011.

[11] Perkins G , Sahajwalla V . A Numerical Study of the Effects of Operating Conditions and Coal Properties on Cavity Growth in Underground Coal Gasification[J]. Energy & Fuels, 2006, 20(2):81 - 88.

[12] Luo Y, Coertzen M, Dumble S. Comparison of UCG cavity growth with CFD model predictions. In: Proceedings of the 7th international conference on CFD in the minerals and process industries CSIRO, melbourne, Australia; December 2009. p. 9e11.

[13] Seifi M, Chen Z, Abedi J. Numerical simulation of underground coal gasification using the CRIP method. Can J Chem Eng 2011;89(6):1528-35

[14] Samdani G, Aghalayam P , Ganesh A , et al. A process model for underground coal gasification – Part-I: Cavity growth[J]. Fuel, 2016.

[15] Samdani G , Aghalayam P , Ganesh A , et al. A process model for underground coal gasification – Part-II growth of outflow channel[J]. Fuel, 2016, 181:587-599.

[16] Sarndani G , Aghalayam P , Ganesh A , et al. A process model for underground coal gasification – Part-III: Parametric studies and UCG process performance[J]. Fuel, 2018, 234(DEC.15):392-405.

[17] Aj A ,Fs A ,Mn B . A new model for evaluation of cavity shape and volume during Underground Coal Gasification process - ScienceDirect[J]. Energy, 2018, 148:756-765.

[18] G. J , Harloff. Underground Coal Gasification Cavity Growth Model[J]. Journal of Energy, 1983.

[19] Daggupati S , Mandapati R N , Mahajani S M , et al. Laboratory studies on cavity growth and product gas composition in the context of underground coal gasification[J]. Energy, 2011, 36(3):1776-1784.

[20] Yang Lanhe, Liang Jie. TEM detection method in the combustion air area of underground coal gasification [J]. Journal of Nanjing University of Science and Technology, 2001, 25(2):5.

[21] Chen Qihui, Liang Jie, Yu Li, et al. Research on detection of underground gasification combustion zone and moving speed by radon measurement method [J]. Journal of Shandong Jianzhu University, 2008, 24(3):5.

[22] Jinghua Liu, Xingtai Wang, Gang Tian, Zhuwen Wang. Dynamic monitoring of coal underground gasification goafs by radioactive radon measurement [J]. Geophysical and Geochemical Exploration,2000(02):92-98.

[23] Najafi M , Jalali S , Khalokakaie R , et al. Prediction of cavity growth rate during underground coal gasification using multiple regression analysis[J]. International Journal of Coal Science & Technology, 2015, 2(004):318-324.

[24] Prabu V , Jayanti S . Simulation of cavity formation in underground coal gasification using bore hole combustion experiments[J]. Energy, 2011, 36(10):5854-5864.

[25] Prabu V , Jayanti S . Heat-affected zone analysis of high ash coals during ex situ experimental simulation of underground coal gasification[J]. Fuel, 2014, 123(may 1):167-174.

[26] Jowkar A , Sereshki F , Najafi M . Numerical simulation of UCG process with the aim of increasing calorific value of syngas[J]. International Journal of Coal Science & Technology, 2020, 7(1):196-207.

[27] Javed S B , Uppal A A , Bhatti A I , et al. Prediction and parametric analysis of cavity growth for the underground coal gasification project Thar[J]. Energy, 2019, 172(APR.1):1277-1290.

[28] Su F Q , Itakura K I , Deguchi G , et al. Monitoring of coal fracturing in underground coal gasification by acoustic emission techniques[J]. Applied Energy, 2017, 189(MAR.1):142-156.

[29] Su F Q , Hamanaka A , Itakura K I , et al. Monitoring and evaluation of simulated underground coal gasification in an ex-situ experimental artificial coal seam system[J]. Applied Energy, 2018, 223(AUG.1):82-92.

[30] Yang Lanhe. Research on the characteristics and influencing variables of the "three zones" of underground coal gasification [J]. Journal of Nanjing University of Science and Technology (Natural Science Edition), 2001(05):533-537.DOI:10.14177/j. cnki.32-1397n.2001.05.021.

[31] Ekneligoda T C , Marshall A M . A coupled thermal-mechanical numerical model of underground coal gasification (UCG) including spontaneous coal combustion and its effects[J]. International Journal of Coal Geology, 2018, 199:31-38.

[32] Xu B , Yang M , Xing B , et al. Removal of pollutants from aqueous solutions by coals and residual cokes obtained from simulated underground coal gasification experiments[J]. Fuel, 2021, 292(4):120292.

[33] Ma Ailing, Chen Lunjian, Xu Bing. Study on the physicochemical properties of residues in the "three belts" of underground coal gasification [J]. Coal Science and Technology, 2019, 47(11): 217-223. DOI: 10.13199/j .cnki.cst.2019.11.031

Study on the monitoring method of cavity growth in underground coal gasification under laboratory conditions

Fa-qiang Su[a,b], Jun-bo Wu[a], Tao-Zhang[a], Qi-chao Deng[a], Yi-he Yu[a,b,]*, Akihiro Hamanaka[c], Meng-Jia Dai[a], Jun-Nan Yang[a],Xiao-long He[a]

[a] School of Energy Science and Engineering, Henan Polytechnic University, Jiaozuo, Henan, 454-003, China

[b] State Collaborative Innovation Center of Coal Work Safety and Clean-efficiency Utilization, Henan Polytechnic University, Jiaozuo, Henan, 454-003, China

[c] Department of Earth Resources Engineering, Kyushu University, 744 Motooka, Nishi-ku, Fukuoka 819-0395, Japan

* Correspondence: yyhcmsj@hpu.edu.cn

Abstract: The growth state of the combustion cavity during underground coal gasification (UCG) affects the gasification process's efficiency, stability, and accurate monitoring and control. In this study, a simulation experiment of UCG was performed, and a horizontal coaxial gasification channel was drilled based on the constructed artificial coal seam (lump coal). Oxygen and air are used as gasification agents to provide a sufficient temperature field to sustain the gasification process. The effect of different positions of the injection pipe port on the growth of the gasification combustion cavity was studied. Moreover, the derivation of the gasification zone during UCG was developed using stratified temperature monitoring and acoustic emission damage monitoring. After the experiment, the artificial coal seam was cut to obtain the profile shape of the combustion cavity, which was compared with the temperature and acoustic emission monitoring results. The results show that the temperature distribution results in the coal seam and the calibration results of the acoustic emission source during horizontal coaxial UCG are consistent with the two-dimensional and three-dimensional combustion cavities reconstructed by the profile. Thus, the effectiveness of stratified temperature monitoring and acoustic emission monitoring to infer the gasification combustion cavity is proven.

Keywords: Underground coal gasification; Combustion cavity; Stratification temperature; Acoustic emission; Profile

1 Introduction

Underground coal gasification (UCG) is a new type of mining method that involves the process of burning coal stored underground to produce combustible gas in a controlled manner. This process consists of excavating coal from the ground to the coal seam, establishing a gasification channel in the coal seam, injecting gasification agents into the coal seam through the gas injection well, letting the coal go through a series of processes such as oxidation and reduction, and generating gas that is finally discharged to the ground through the production well [1]. During UCG, as gasification progresses, the flow channel between the injection well and the production well expands with the consumption of the coal seam, and the resulting space is called the combustion cavity. Combustion cavity formation is one of the most critical links in the UCG process [2]. The growth of the combustion cavity is a dynamic process; it is the continuous expansion of the gasification channel with combustion and oxidation, accompanied by the generation of many cracks. If the cracks are too large, they may cause excessive damage to the rock strata above the gasification area, and the cracks around the gasification area may also run through the surface or underground water, resulting in gas leakage and environmental pollution and affecting the regular progress of underground coal gasification [3]. For example, in the 1970s and 1980s, dozens of UCG tests were conducted in the United States. Three tests (HoeCreek I, II, and III) at HoeCreek, Wyoming, produced surrounding water pollution and surface subsidence [4-6]. Therefore, monitoring the growth of the combustion cavity during the UCG process is very important for the stability of the upper part of the geological structure and the state of the surrounding environment [7].

Due to the vital role of combustion cavity growth in the UCG process, many scholars have used a variety of modeling methods to study this growth [8-10]. For example, Perkins and Sahajawalla proposed a one-dimensional model to study the effects of different operating parameters on combustion cavity growth in the UCG process, and the results showed that coal characteristics such as temperature, water flow, gas pressure, ash content, and carbon constant value have the most significant influence on the growth rate of the combustion cavity [11]. Luo et al. proposed a two-dimensional mathematical model to study combustion cavity growth in the UCG process, and the results showed that the proposed model could predict the combustion cavity shape, temperature distribution, and amount of gasified coal [12]. Seifi et al. proposed a 3D simulation of the UCG process, which was shown to predict the cavity shape and temperature distribution [13]. Samdani et al. developed a CFD model to simulate the UCG process. In the first stage, when the coal near the injection well is consumed, the cavity grows in the vertical direction, and in the second stage, the cavity grows in the horizontal direction. The results show that the model can predict the combustion cavity growth rate [14-16]. Amin Jowkar et al. introduced the constitutive function equation in simulating UCG. The results show that the constitutive function equation can predict the expansion of the combustion cavity [17]. Eddy et al. established a two-dimensional model to describe the effects of natural convection and forced convection on heat and mass transfer on the sidewall of the combustion cavity [18]. Various research methods based on mathematical models and simulations have revealed the development of combustion cavities. However, some variable factors have been ignored in the simulation, such as the rock and soil mass, which are not homogeneous and isotropic, and the effect of seepage on the temperature field. In addition, coal samples are also heterogeneous, and the UCG process involves complex physical processes, homogeneous and heterogeneous chemical reactions, complex flow patterns of reaction gases, heat and mass transport, and thermal-mechanical failure of coal seams [19]. Moreover, the simulation only considers some specific factors. Thus, the accuracy of the methods cannot be verified since there are no experimental data for comparison.

As a result, some scholars have conducted experiments to analyze the growth rate of combustion cavities. Yang et al. used the transient electromagnetic method to detect the combustion cavity and predicted the boundary of the combustion cavity according to the change law of electrical impedance of coal and surrounding rock under different temperature conditions [20]. Chen et al. predicted the flameworking face's position and the combustion cavity's scope in underground coal gasification by the radioactive radon method. The prediction is mainly based on the enrichment characteristics of radioactive elements in coal before and after combustion and the migration law of radon gas at different temperatures and pressures in the gasification zone [21]. In the underground gasification of the Tangshan Liuzhuang Coal Mine, radioactive radon gas was used to monitor the movement of the gasification working face and the expansion range of the combustion cavity [22]. Mehdi et al. developed a simple model to predict the combustion cavity expansion rate using a nonlinear regression analysis method based on data from UCG field experiments [23]. Prabu et al. designed a gasification device with a special type of wood as a carrier to simulate the expansion of the combustion cavity during the gasification process; however, in this experiment, stopping the gasification process several times and disassembling the model to observe and evaluate the combustion zone was necessary. The results show that the cavity formation rate and cavity shape are significantly affected by the oxidant flow rate [24-25]. Jowkar et al. used COMSOL software to establish a model to predict the combustion cavity's shape and volume and determine the gas's calorific value and composition [26]. Javed et al. parameterized the three-dimensional axisymmetric cavitation simulation model, studied the influence of various operating parameters on the cavitation expansion, and predicted the cavitation expansion and its interaction with overburden [27]. Su et al. used acoustic emission monitoring combined with temperature monitoring and product gas composition analysis to monitor cavity growth during the UCG process [28-29]. In the above studies on the growth of the combustion cavity, the combustion cavity is indirectly inverted by monitoring the signals generated during the UCG process, and there is no direct means to investigate the expansion of the combustion cavity.

In this paper, the underground gasification system of a horizontal coaxial hole-type gasification channel is used to simulate underground coal gasification. In addition, temperature sensors and acoustic emission sensors are arranged in layers to monitor the temperature and acoustic emission signal inside the coal sample during the gasification process. At the end of the experiment, gypsum slurry was filled into the combustion cavity, and after it was solidified and formed, the two-dimensional section morphology of the gasification coal sample was observed layer by layer, and the three-dimensional morphology of the gasification combustion cavity was constructed. Therefore, the variation law of acoustic emission and temperature in the process of gasification combustion cavity expansion is analyzed, and the shape and size of the combustion cavity can be predicted and evaluated based on acoustic emission and temperature monitoring data.

2 UCG experimental model

2.1 UCG experimental system

The UCG experiment was carried out in a steel container filled with large coals. To ensure airtightness, refractory cement was used to fill the voids around the steel container. The UCG simulation experiment system is mainly composed of the main gasifier, the gasification agent injection system, the acoustic emission (AE) monitoring system, the temperature monitoring system, and the product gas analysis system. The schematic diagram is shown in Fig 1.

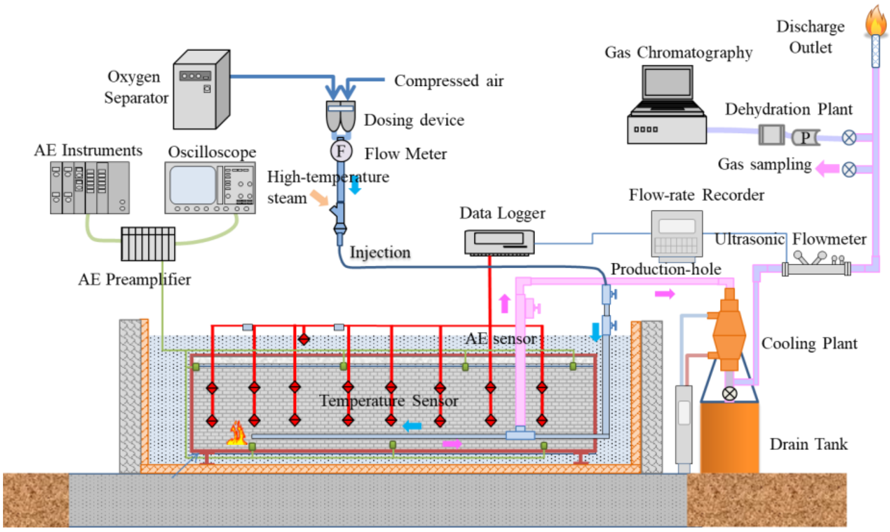

Fig. 1. UCG simulation experiment system

2.2 Coal sample

During the heating process of the coal sample in which the coal seam is gasified and burned along the bedding plane, the gasification zone is more likely to expand. Therefore, when constructing a horizontal coaxial UCG model gasifier, the gasification channel is set parallel to the bedding plane of the coal sample. In the experiment, a coal seam of 2700 × 550 × 600 mm (length × width × height) was constructed by combining coal samples with a length and width greater than 600 mm, as shown in Fig. 2(a). Cement and pulverized coal (1:10 ratio) filled the gaps between the coals, as shown in Fig. 2(b). The outer wall of the coal seam is covered with refractory cement to prevent heat release and gas leakage, as shown in Fig. 2(c). Table 1 shows the proximate and ultimate analysis of coal samples.

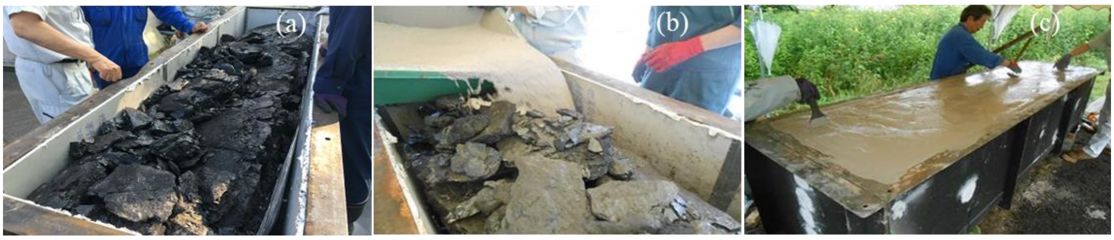

Fig. 2. Construction of UCG model

Table 1. Proximate analysis and ultimate analysis of coal samples

Calorific value (MJ/kg)	Proximate analysis (wt%)				Ultimate analysis (wt%)				
	Moisture	Ash	Volatiles	Fixed carbon	C	H	N	S	O
32.12	2.10	4.30	43.10	50.50	78.40	5.74	1.44	0.07	9.94

2.3 Arrangement of gasification channels

The vertical section of the experimental simulation system is shown in Fig. 3. A horizontal coaxial gasification passage 45 mm in diameter and 2600 mm in length was drilled with a 45 mm diameter auger at a height of 100 mm from the bottom of the steel vessel. Taking pictures of the inside of the gasification channel with an endoscope, it can be seen that coal exists around the gasification channel of each section, and the hole wall is kept in good condition and does not collapse, as shown in Fig. 4.

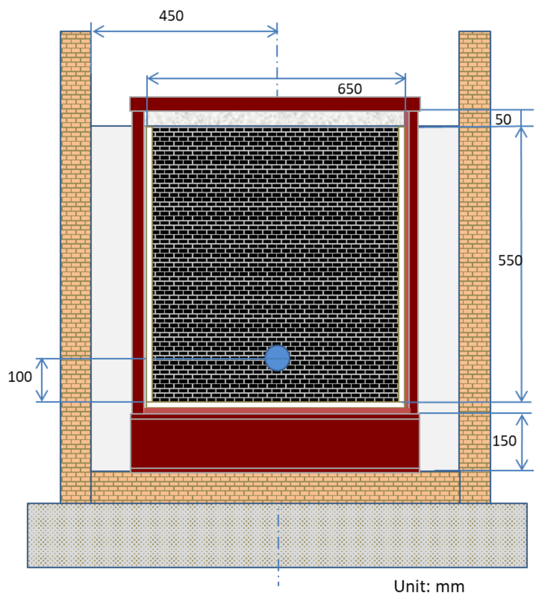

Fig. 3. Vertical section view of the gasifier

2500 mm from drilling 1600 mm from drilling 700 mm from drilling

Fig. 4. Inside the gasification channel

The main gasifier in the experimental system is installed in a steel container, and the gasification channel is a horizontal coaxial type. An injection pipe is inserted from the drill hole, and a mixed gas (gasification agent) of oxygen and air can be injected from the inside of the injection pipe. By continuously injecting a certain amount of gasification agent, combustion and gasification can be carried out inside the coal seam. The generated gas is guided from the outside of the injection pipe and the hole wall to the production pipe connected to the nozzle for later analysis and processing. To analyze the spatial distribution of temperature, acoustic emission and combustion cavity over time during the gasification process, a two-dimensional coordinate system was established with the bottom of the gasification channel as the origin, as shown in Fig. 5.

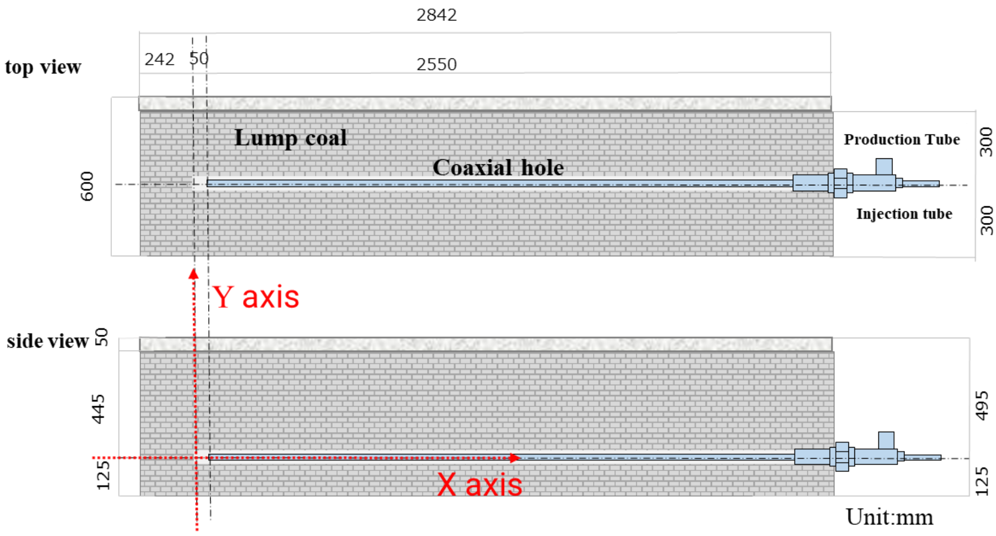

Fig. 5. Horizontal coaxial gasification channel

2.4 Sensor arrangement

2.4.1 Temperature sensor

Fig. 6 shows a schematic diagram of the buried position of each temperature sensor. Starting from the position 50 mm away from the bottom of the gasification channel, temperature sensors T1-1~T1-8 are placed directly above the gasification channel, temperature sensors T2-1~T2-8 are placed 150 mm above the gasification channel, and temperature sensors T3-1~T3-8 are placed 300 mm above the gasification channel. The horizontal interval between adjacent sensors is 300 mm. T4-1~T4-4 are embedded in 100 mm of the negative half-axis of the X-axis, with a height interval of 100 mm. Temperature sensors T4-1 to T4-1 are used to observe the temperature distribution at different heights. Fig. 7 shows the temperature sensor embedded on the top and side of the steel container.

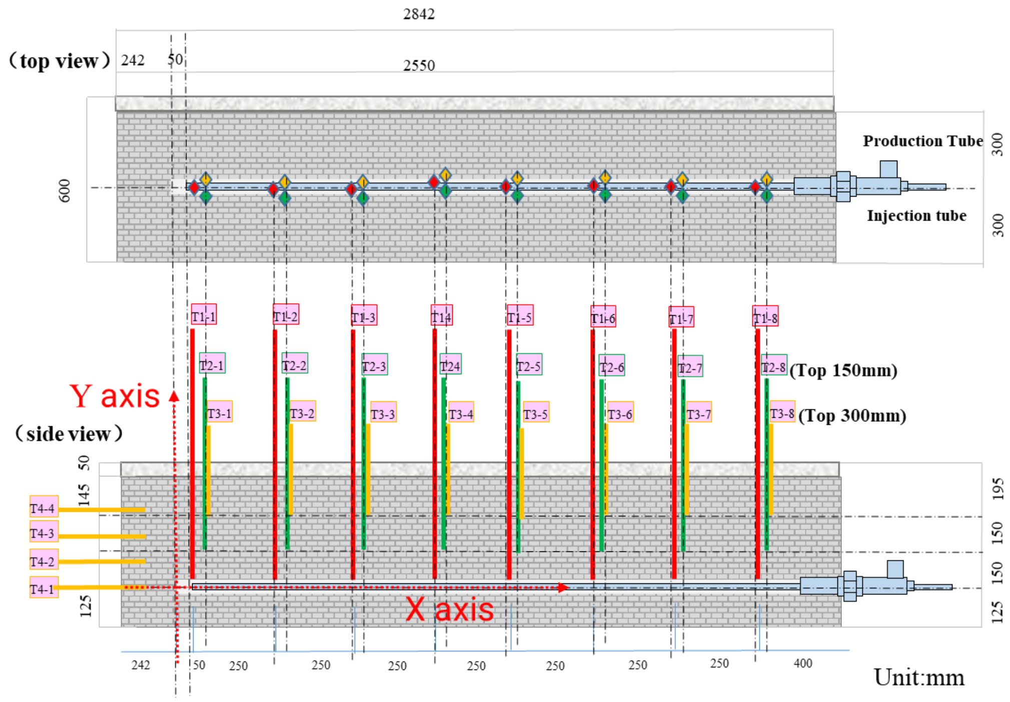

Fig. 6. Layout of temperature sensors

Fig. 7. The temperature sensor buried above and to the sides of the steel container

2.4.2 Acoustic emission (AE) sensor

During the UCG process, the high temperature causes thermal stress inside the coal seam, and microcracks occur. Acoustic emission signals are generated in the gasification process, and the faster the temperature change of the coal sample is, the more active the acoustic emission activity is [25]. To monitor the expansion of the surrounding damage area during the combustion process, acoustic emission sensors that detect minor damage were arranged around the lump coal sample.

In this experiment, all acoustic emission sensors are installed on the side of the steel container shell of the gasifier. Multiple 8 mm diameter holes were drilled from the steel vessel shell, the waveguide rod was inserted and the end of the waveguide rod was ensured to enter the coal seam. The gap was filled, the waveguide rod was fixed with refractory glue, and the gap between the coal and the steel vessel shell was filled with heat-resistant cement. After the cement is cured, the acoustic emission sensor is mounted on the waveguide rod. Fig. 8 is a schematic diagram of the configuration of the acoustic emission sensor. Fig. 9 shows the setting method of the acoustic emission sensor. Fig. 10 is a schematic diagram of the installation of the acoustic emission sensor on the sidewall of the steel container.

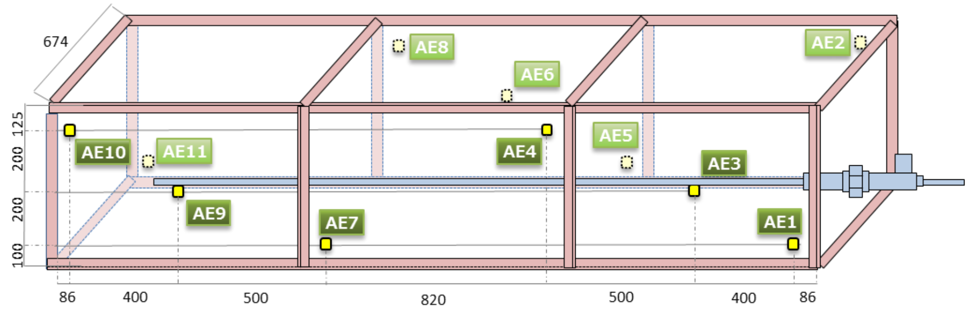

Fig. 8. Configuration diagram of the acoustic emission sensor

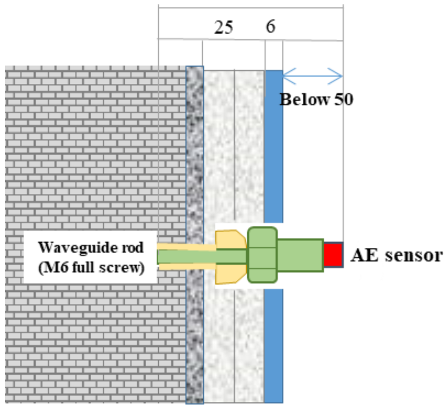

Fig. 9. Setting method of the acoustic emission sensor

Fig. 10. Acoustic emission sensor set on the sidewall of the steel container

2.5 UCG experimental process

In this experiment, the gasification combustion area was changed by moving the position of the injection pipe port. At the beginning of the experiment, the injection pipe port was located 350 mm from the bottom of the gasification channel, that is, Point (350,0). After 24 h, 38 h, 47 h, and 63 h of ignition, the port of the injection pipe was moved several times by 300 mm to the positive half-axis direction of X. Fig. 11 depicts the oxygen injection flow rate and total injection volume per minute during the experiment. The total flow rate of 0~24 h of injection was set to 30 L/min, of which oxygen was 15 L/min, and the total flow rate of 24~73 h was increased to 40 L/min, of which oxygen was 20 L/min. After 73 h, nitrogen and carbon dioxide were injected into the gasifier to extinguish the fire. The experimental process was divided into six stages according to the injection pipe port and the gasification agent flow rate. Moreover, the time points were 0~24 h, 24~38 h, 38~47 h, 47~63 h, 63~73 h, and 73~83 h.

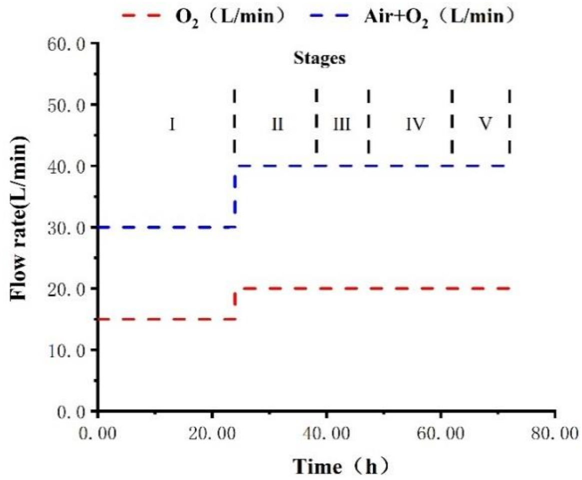

Fig. 11. Oxygen injection amount and total injection amount in the experiment

The pressure was recorded after successful ignition, which produced a large amount of flammable gas. The pressure was recorded after successful ignition, which produced a large amount of flammable gas. During the experiment, the internal pressure of the cavity was in a positive state, fluctuating in the range of 0.06~0.10MPa, as shown in Fig. 12. Therefore, the interior of the cavity is in a stable state, which provides reliability for subsequent experimental data analysis. There was no evident gas leakage during the experiment, indicating that the refractory cement and cement have good sealing performance.

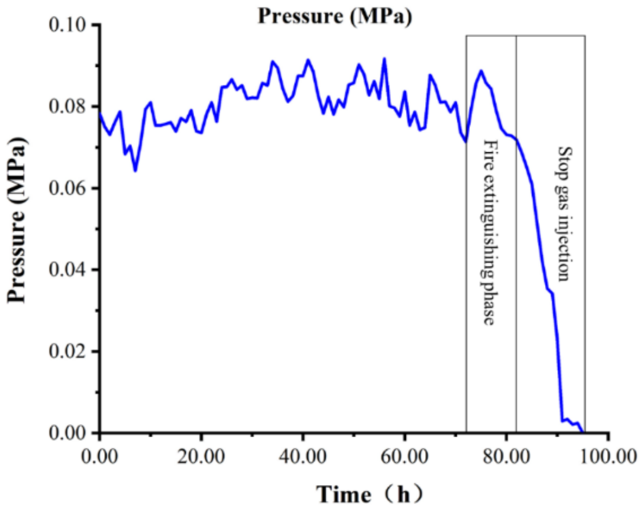

Fig. 12. Pressure changes during the experiment

3 Experimental results

3.1 Temperature change during gasification

Fig. 13 shows the temperature changes of temperature sensors T1-1 to T1-8, T2-1 to T2-8, T3-1 to T3-8, and T4-1 to T4-4 during the experiment. The coordinates of the injection pipe port at each stage of the experiment are shown in Table 2. The coordinate calibration of the temperature sensor is shown in Table 3.

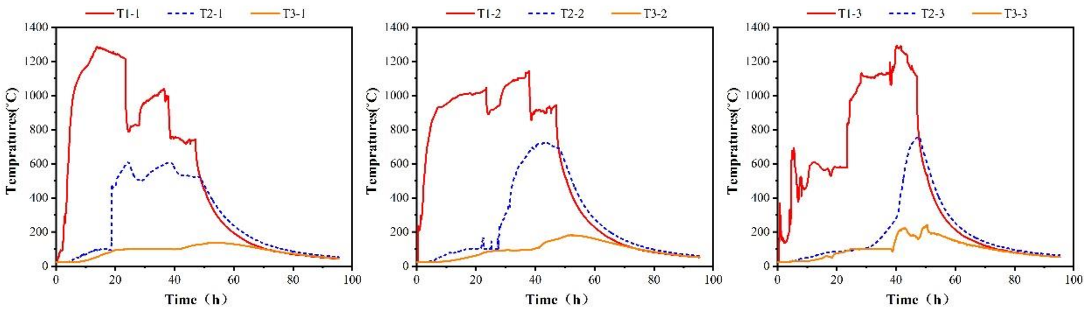

(a) T1-1~T1-3, T2-1~T2-3 and T3-1~T3-3

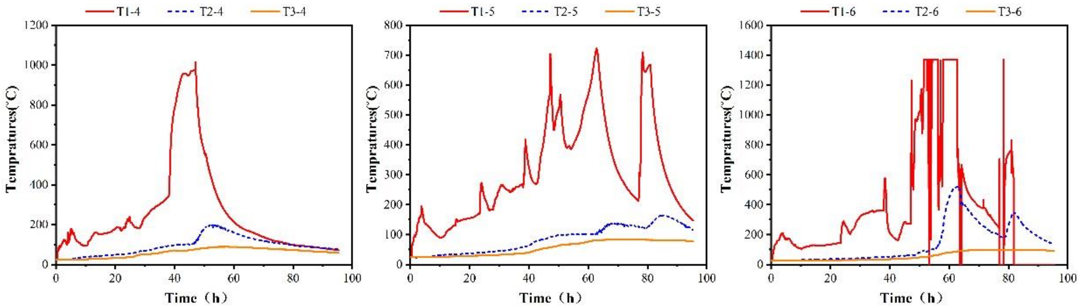

(b) T1-4~T1-6, T2-4~T2-6 and T3-4~T3-6

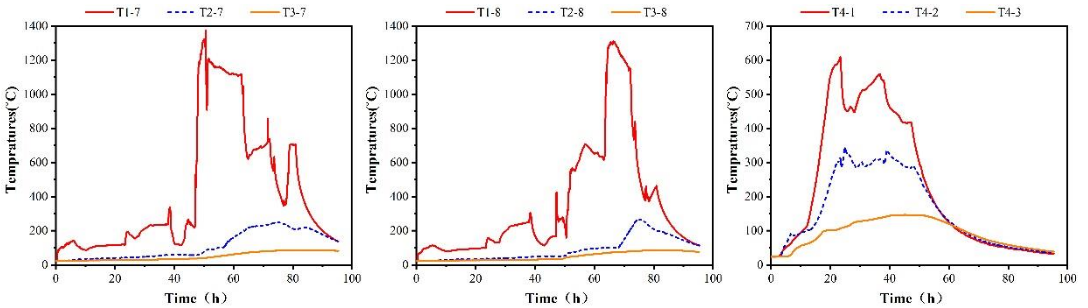

(c) T1-7~T1-8, T2-7~T2-8, T3-7~T3-8 and T4-1~T4-3

Fig. 13. Variation in temperature in the coal sample with time

Table 2. Coordinate calibration of the injection pipe port at each stage of the experiment (taking the bottom of the gasification channel as the coordinate origin)

Time(h)	0~24	24~38	38~47	47~63	63~73	73~83
Stage	Ⅰ	Ⅱ	Ⅲ	Ⅳ	Ⅴ	Ⅵ
Coordinates	350,0	650,0	950,0	1250,0	1550,0	1550,0

Table 3. Coordinate calibration of the temperature sensor (taking the bottom of the gasification channel as the coordinate origin)

	1	2	3	4	5	6	7	8
T1~	50,0	350,0	650,0	950,0	1250,0	1550,0	1850,0	2150,0
T2~	50,150	350,150	650,150	950,150	1250,150	1550,150	1850,150	2150,150
T3~	50,300	350,300	650,300	950,300	1250,300	1550,300	1850,300	2150,300
T4~	-100,0	-100,100	-100,200	-100,300				

The port of the injection pipe starts to ignite at X=350 mm, and after 24 h, 38 h, 47 h, and 63 h, the port of the injection pipe moves to the positive half-axis of X at a scale of 300 mm.

The temperature sensors T1-1~T1-8 are arranged at the same level as the gasification channel. The temperatures of T1-1 and T1-2 sharply rose after ignition. The temperature of T1-3 sharply increased after 24 h and reached a local temperature peak at 28 h. As the experiment progressed, the high-temperature area moved to the positive semiaxis of the x-axis. After 38 h, the temperature of T1-4 sharply rose, reaching a local peak at 42 h. After 47 h, the temperatures of T1-5, T1-6, and T1-7 sharply increased. The temperature of T1-5~T1-7 reached a local peak at 51 h. The temperature of T1-8 sharply rose after 63 h and reached a local peak at 67 h. The change in the position of the injection pipe port was the same as the time node when the temperature of T1-1~T1-8 began to rise. With the injection pipe's movement, the gasification agent's supply area changed, and the gasification area moved accordingly. Therefore, by moving the position of the injection pipe port, the combustion gasification reaction of the unreacted coal region can be promoted, and the gasification region can be guided to expand in a predetermined direction. In addition, the flow rate and composition of the gasification agent injected within 24~73 h were the same. The coal violently burned within approximately four hours after the injection pipe was moved, and the temperature rose faster. The local temperature peaked at four hours, indicating that after the continuous injection of the gasification agent for four hours, the combustion was the most intense.

The maximum temperature of temperature sensors T1-4 and T1-5 in the middle of the gasification channel is approximately 800°C, while the maximum temperature of T1-1~T1-3 and T1-6~T1-8 at both ends exceeds 1000°C. Therefore, the scale of coal combustion is smaller in the area containing temperature sensors T1-4 and T1-5 than in the other areas. Temperature sensors T2-1 to T2-8 are embedded with the coordinate axis Y= 150 mm. The maximum temperature of T2-4 to T2-5 in the middle of the gasification passage is below 300°C, but the maximum temperature of T2-1 to T2-3 and T2-6 on both sides reaches 600°C to 800°C. This phenomenon shows that the degree of gasification is small between X=950~1250 mm in the middle of the gasification channel, and the upper boundary of the central coalbed gasification area is not developed to 150 mm above.

Temperature sensors T3-1 ~ T3-8 are buried at the coordinate axis Y = 300 mm, and the overall maximum temperature is below 200°C. There is no combustion in the entire area at this height, so the upper boundary of the artificial coalbed gasification area is located on the coordinate axis Y = in the range of 150 mm to 300 mm.

The temperature sensor T4-1 is buried at coordinate axis X= -100 mm, and its maximum temperature exceeds 600°C; T4-2 is buried at 100 mm above T4-1, and its maximum temperature exceeds 300°C. Thus, the left boundary of the gasification area is located at coordinate axis X= -100 mm.

3.2 Correlation analysis between high-temperature regions and acoustic emissions

For convenience, X=-150~950 mm is the left side of the artificial coal seam, X=950~1250 mm is the middle of the artificial coal seam, and X=1250~2350 mm is the right side of the artificial coal seam. The temperature data were analyzed and processed in combination with the position of the temperature sensor, and the expansion process of the high-temperature region of the gasification zone during the experiment was obtained, as shown in Fig. 14.

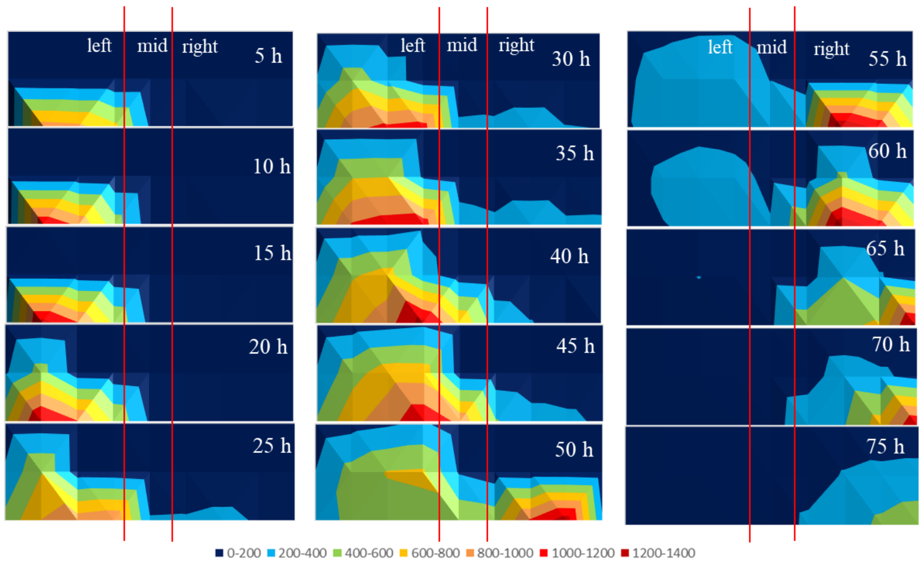

Fig. 14. High-temperature area expansion diagram

From 0~24 h, the temperature on the left side of the coal seam rapidly increased after ignition was successful. From 24~38 h, the overall temperature gradually increased, developed from the left side of the coal seam, gradually expanded to the middle of the coal seam, and finally reached the highest temperature on the left side. This shows that the gasification region of 0~38 h is on the left side of the coal seam. From 38~63 h, the temperature in the central area gradually increased, and the temperature in the left area gradually decreased. The high-temperature field migrated to the right side across the middle of the coal seam and finally reached the highest temperature on the right side. This shows that the 38~63 h gasification area is on the right side of the artificial coal seam. From 63~73 h, the temperature of the gasification area on the right side gradually decreased, and the high-temperature field migrated to the right boundary of the coal seam. In short, the distribution range of high-temperature areas on the left side of the coal seam is more extensive than that on the right side, and the low-temperature areas are concentrated in the middle and upper parts of the coal seam.

The calibration results of the AE source and the distribution results of the highest temperature in the coal seam at the five stages are shown in Fig. 15. In the distribution diagram of the AE source calibration results, different colors represent the acoustic emission events generated in different stages, the position of the ball indicates the location of the acoustic emission, and its size indicates the relative energy, that is, the size of the damage scale.

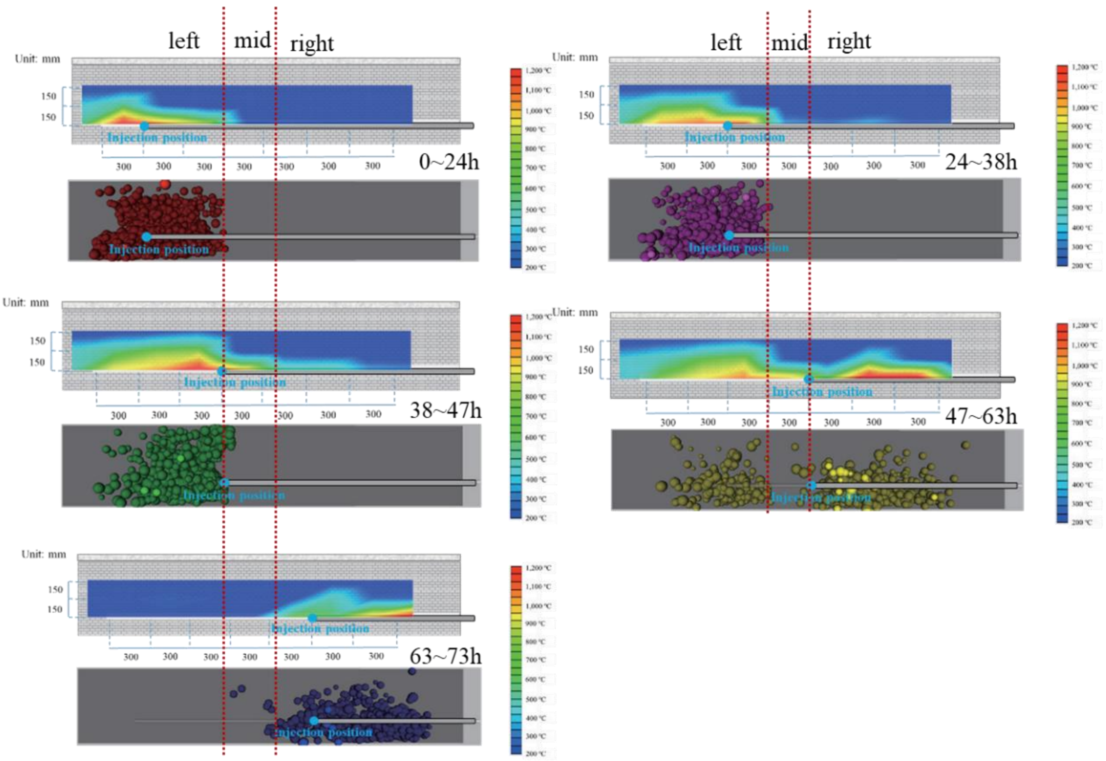

Fig. 15. AE source calibration results and maximum temperature distribution in the coal seam (side view)

From 0~47 h (I~III), many AE events were generated from the bottom to the top of the coal seam. However, within 47~73 h (IV~ V), many AE events occurred from the bottom to the middle of the coal seam, and fewer occurred above. This trend is consistent with the fact that the high-temperature area of the temperature profile extends in the upper part of the left side, while the high-temperature area is lower on the right side.

Within 0~47 h (Ⅰ~Ⅲ), on the left side of the coal seam, the high-temperature area expands over a wide range, and the AE source is also widely distributed.

Within 47~63 h (Ⅳ~ Ⅴ), on the left side of the coal seam, the distribution of high-temperature areas is small, and the distribution of AE hypocenters is also scattered. The temperature rise in the middle of the coal seam is tiny, and the AE source is hardly calibrated. On the right side of the coal seam, the high-temperature region is enlarged relative to the left side, and the AE source is widely distributed relative to the left side.

Throughout the experiment, the position of the AE shifted with the movement of the high-temperature region. From 0~73 h, the high-temperature area gradually moved to the right side of the coal seam, and the AE source calibration results also showed the same moving trend.

3.3. Gasification zone and combustion cavity growth process

3.3.1 Profile of the gasified coal sample

After the experiment, consisting of several hours of nitrogen and carbon dioxide to extinguish the fire, three vertical holes were drilled from the artificial coal seam to the gasification channel. The gypsum solution was poured into the lump coal sample. After the gypsum solidified, the block coal sample was cut to observe the condition of the vertical section. The artificial coal seam was cut at intervals of 100 mm, and the expansion of the gasification area on the vertical section was observed. Fig. 16 shows the positions of each section (Sections 5, 14, and 23 are the drilling positions). The coordinates of the sections are shown in Table 4.

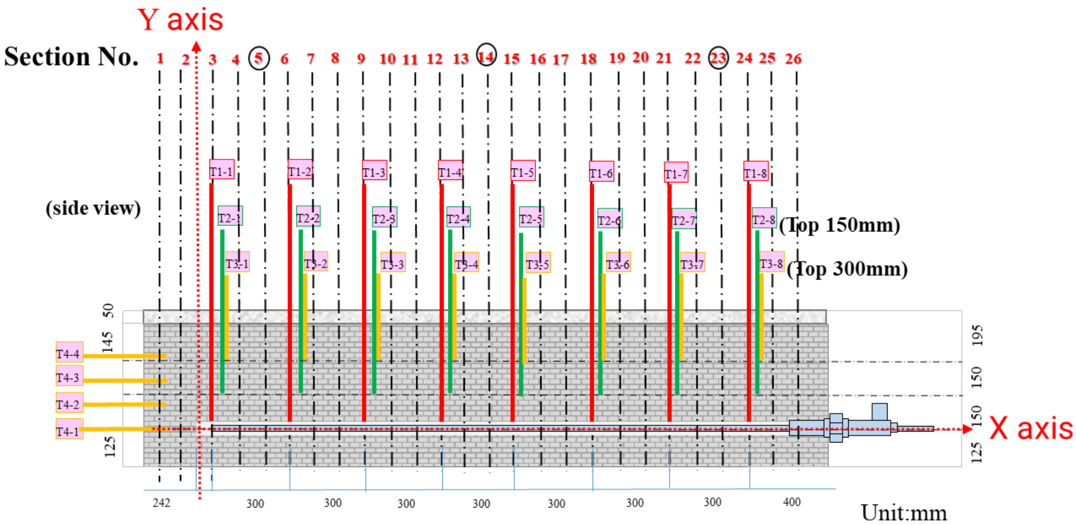

Fig. 16. Profile location, profile number and configuration of the temperature sensor (side view)

Table 4. Coordinate calibration of the section (taking the bottom of the gasification channel as the coordinate origin)

No.	1	2	3	4	5	6	7	8	9	10	11	12	13
X=	-150	-50	50	150	250	350	450	550	650	750	850	950	1050
No.	14	15	16	17	18	19	20	21	22	23	24	25	26
X=	1150	1250	1350	1450	1550	1650	1750	1850	1950	2050	2150	2250	2350

After grouting the cavity formed by the artificial coal seam gasification process, the cut section is shown in Fig. 17. The figure marked T1-1~T1-8 is the section of the buried temperature sensor. In Profiles No. 5, No. 14, and No. 23, the vertically extending white portion is the trace of drilling when gypsum was injected. Sampling and analysis of the residues in the section is performed, similar components are classified into the same area, and each section is roughly divided into the combustion cavity, the gasification area, the unreacted coal area and the cement-filled area, as shown in Fig. 18.

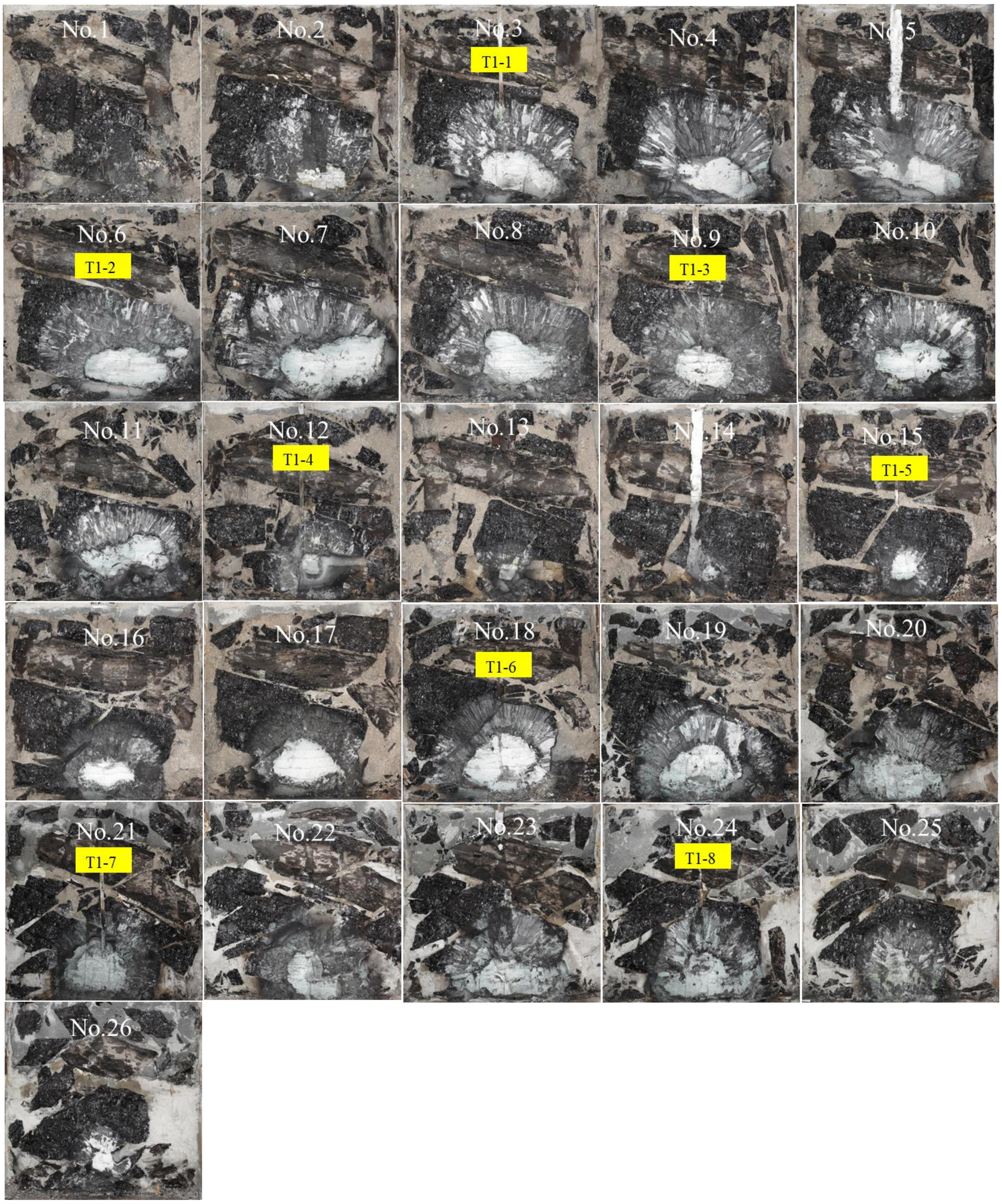

Fig. 17. Profiles after grouting the cavity formed by the artificial coal seam gasification process

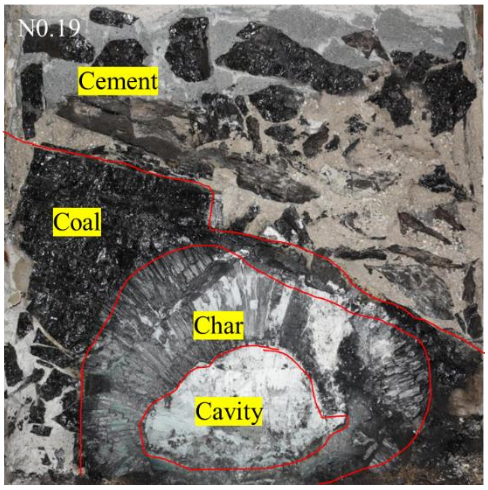

Fig. 18. Distribution of different regions

According to the temperature of the coal seam, chemical reaction and product gas composition, the underground gasification process is divided into an oxidation zone, reduction zone and dry distillation zone along the gasification channel [30], as shown in Fig. 19. In the oxidation zone, carbon combustion mainly occurs, releasing much heat, and the temperature is above 900°C. Adjacent to the oxidation zone is the reduction zone. The gas flow generated in the oxidation zone reaches the reduction zone along the gasification channel, the heat generated makes the coal seam in the reduction zone in a hot state, and the temperature is between 550 and 900°C. The dry distillation zone follows the reduction zone. The oxygen-free high-temperature gas flow produces pyrolysis on the coal in the dry distillation zone to promote water analysis and volatilization in the coal. The temperature is between 200 and 550°C. After a series of reactions in the three reaction zones, mixed gas with combustible components, mainly H_2, CH_4 and CO, was generated. With the continuous combustion of the coal seam, the three reaction zones gradually move to the production pipe, and the gasification zone continuously advances in the forward radial and axial directions, thus maintaining the continuous gasification reaction process.

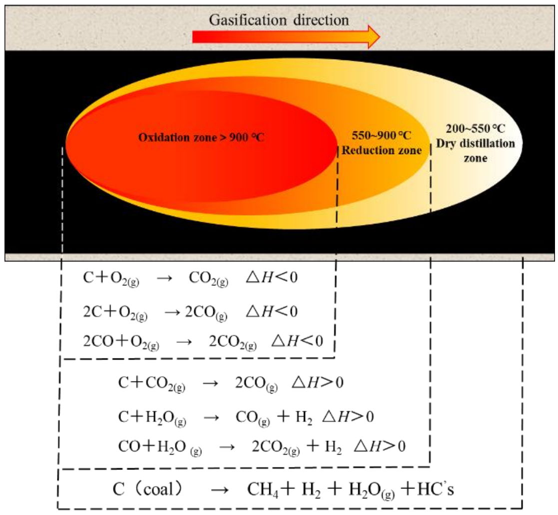

Fig. 19. Schematic diagram of the underground coal gasification reaction process

Due to the different gasification temperatures and the main reactions that occur, the composition of the residues in the three regions must be different. The residue in the oxidation zone is mainly ash, the residue in the reduction zone is mainly gasification residual char, and the residue in the dry distillation zone is mainly pyrolysis semichar [31-32]. Combined with the distribution law of the temperature field in the simulated gasification process, the residues in the three regions were collected along the direction of the gasification channel. The proximate and ultimate analyses of the residue samples are shown in Table 5. Comparing these results with the corresponding initial coals, the ash residue in the oxidation zone contains a small amount of unburned carbon. The char residue in the reduction zone has a lower volatile and slightly higher fixed carbon content than the pyrolysis semichar in the dry distillation zone. This is because the coal seam first goes through drying and retorting, and then gasification occurs at a higher temperature, resulting in a lower volatile content of residual char in the reduction zone and a higher fixed carbon content [33]. In the initial coal of this experiment, element C mainly migrated to the gasification of pure carbon, element H mainly migrated to CH_4 and H_2, element O mainly migrated to CO, CO_2 and residues, and element S and element N mainly migrated to residues.

Table 5. Proximate and ultimate analysis of three zone residuals

	Proximate analysis (wt%)			Ultimate analysis (wt%)				
	Ash	Volatiles	Fixed carbon	C	H	N	S	O
Initial coal	4.30	43.10	50.50	78.40	5.74	1.44	0.07	9.94
Oxidation zone	85.64	78.69	23.65	—	—	—	—	—
Reduction zone	9.65	3.61	97.57	90.47	0.23	0.82	0.08	3.98
Dry distillation zone	7.27	5.86	95.68	90.19	0.34	1.73	0.07	2.54

3.3.2 2D reconstruction of the gasification zone and combustion cavity

(1) Identification of the gasification zone and combustion cavity

A side view was made with gasification channels by using cross-sectional modeling. The combustion cavity, gasification area, unreacted coal area, and cement-filled area are distinguished by color, as shown in Fig. 20 and Fig. 21. In these figures, the white represents the combustion cavity, the gray represents the gasification area, the black represents the unreacted coal area, and the vermilion represents injected cement area. The two-dimensional gasification and combustion cavity constructed according to the distribution map is shown in Fig. 22.

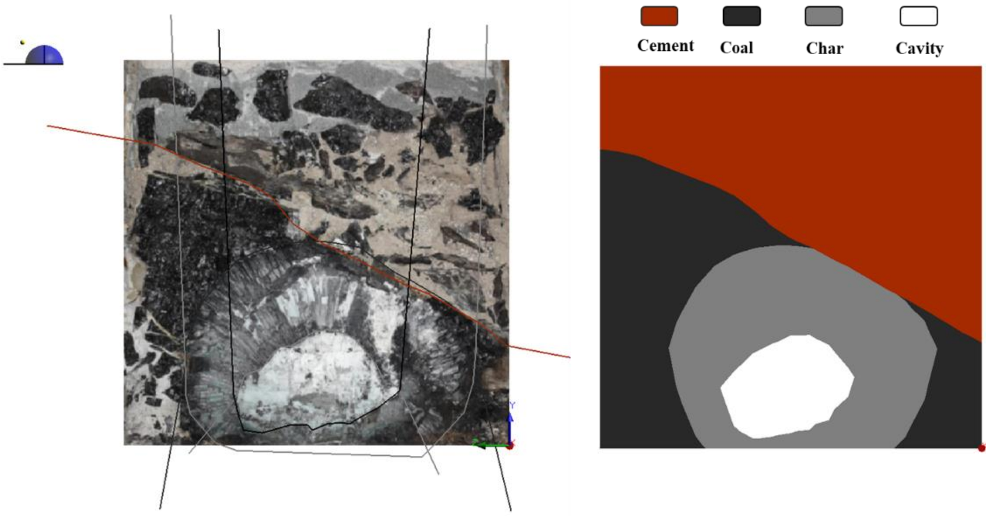

Fig. 20. Side view made by cross-sectional modeling

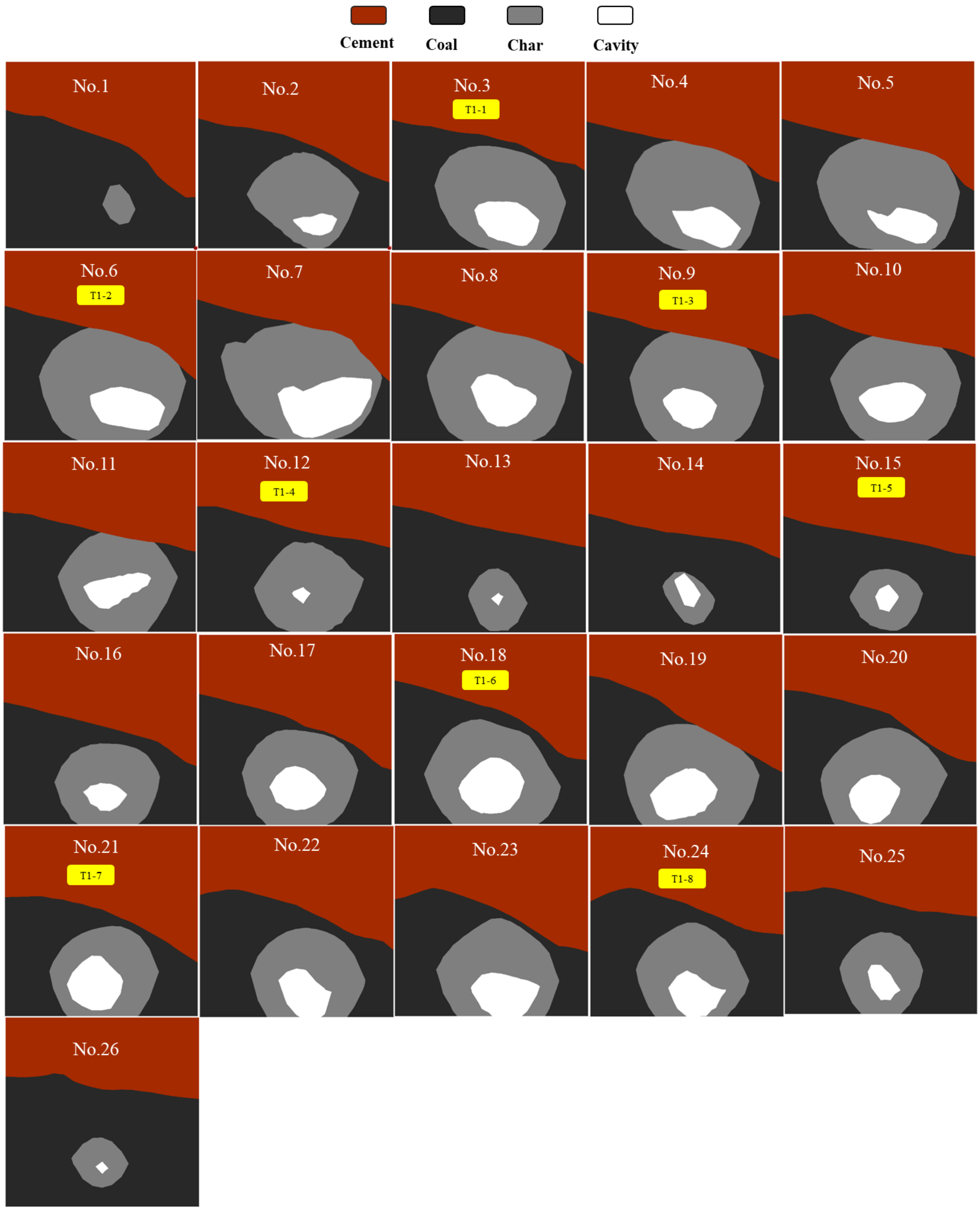

Fig. 21. Profile side view

The section on the left side of the ignition position (the ignition position is X=350 mm) is within -150 mm to -50 mm from the coordinate origin. After ignition is successful, the coal burns to the left and gradually gasifies, and the combustion cavity and gasification area gradually decrease as the distance from the ignition point increases, as shown in Profiles 1 and 2 in Fig. 21.

Within 50 mm to 850 mm from the coordinate origin, the expansion trend of the combustion cavity and the gasification area is stable, and the distribution range is the largest, as shown in Profiles 3 to 11 in Fig. 21. In this range, the maximum temperature inside the gasification channel is 1200-

1500°C, the maximum temperature at 150 mm above the gasification channel is 600-750°C, and the temperature at 300 mm is below 200°C, indicating that the boundary of the gasification region is in the range of Y=150 mm~300 mm. The upper boundary of the gasification zone did not reach Y=300 mm due to the influence of the cement filling layer and rock layer, and the gasification zone may be further expanded if larger coal blocks are present.

Within 950 mm to 1250 mm from the coordinate origin, the expansion range of the combustion cavity and the gasification area is the smallest, as shown in Profiles 12 and 15 in Fig. 21. Profiles 12 to 15 are in the middle of the artificial coal seam. The temperature rise trend in the middle of the high-temperature derivative map of the gasification zone is minimal compared to that of the two sides. The AE source is almost not calibrated and interrupted in the middle. Profile 14 shows that there are many filled cement layers around the gasification channel, and the coal is divided, which restricts the expansion of the gasification area to the outside. There are cement filling layers on the left and right sides and above Profile 15. The maximum temperature of 150 mm above the gasification channel of this profile is approximately 800°C, which is lower than that of the 50 mm~850 mm profile over 1200~1500°C. The presence of cement around profile 15 limits coal combustion.

Within 1350 mm to 1550 mm from the coordinate origin, the expansion range of the combustion cavity and the gasification area gradually increases, as shown in Profiles 16 and 18 in Fig. 21. In the high-temperature derivative map of the gasification zone, the mid-temperate zone is concentrated in this area, and the AE source calibration gradually increases. The maximum temperature 150 mm above the gasification channel is approximately 520°C, indicating that the gasification region extends to the range of Y=150 mm~300 mm but does not reach Y=300 mm. In addition, in the X=1550 mm section, there is a cement filling layer approximately 10 mm wide in the upper left. However, the gasification area extends beyond this cement filling layer into the adjacent coal block.

Within 1650 mm to 2150 mm from the coordinate origin, the expansion trend of the combustion cavity and the gasification area is stable, as shown in Profiles 19 and 24 in Fig. 21. In the high-temperature derivative map of the gasification zone, the high-temperature zone is distributed in this range, and the AE source calibration distribution is concentrated.

Within 2250 mm to 2350 mm from the coordinate origin, the expansion trend of the combustion cavity and the gasification area gradually decreases, as shown in Profiles 25 and 26 in Fig. 21.

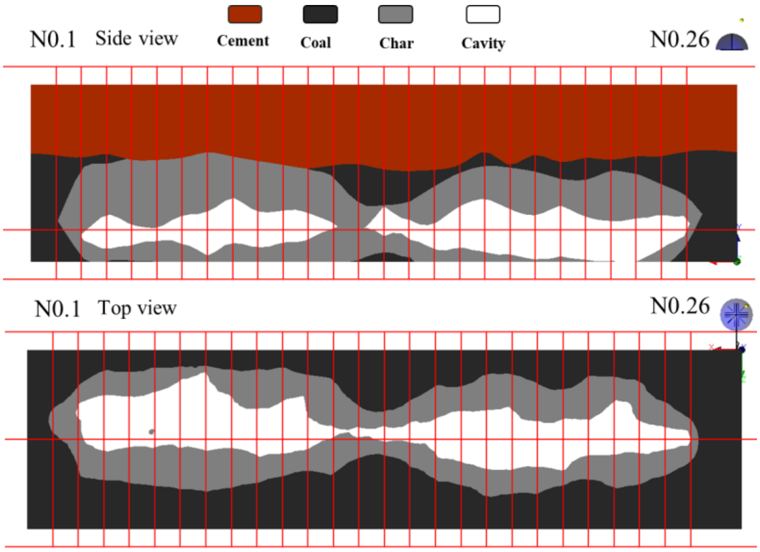

Fig. 22. Two-dimensional gasification and combustion cavity constructed from a cross-sectional distribution map (side and top views)

(2) Relationship between the combustion cavity and the temperature and acoustic emission

Fig. 23 shows the comparison of the two-dimensional section of the combustion cavity, the temperature distribution, and the calibration results of the AE source. First, in the left and suitable regions where the high-temperature region is widely distributed, the AE source distribution range is extensive, and the combustion cavity and gasification region, which are relatively developed in the middle, are fully expanded. The light blue to green (400-600°C) mid-temperature area is widely distributed on the left side. In addition, the AE activity in the left area is more intense. The cutting section shows that the combustion area has expanded to the left boundary of the coal seam. The AE source calibration results and temperature distribution in the coal seam are consistent with the constructed two-dimensional combustion cavity. Second, the temperature rise near the middle of the coal seam is tiny, the high-temperature area is smaller than the range on both sides, and AE events are rarely generated.

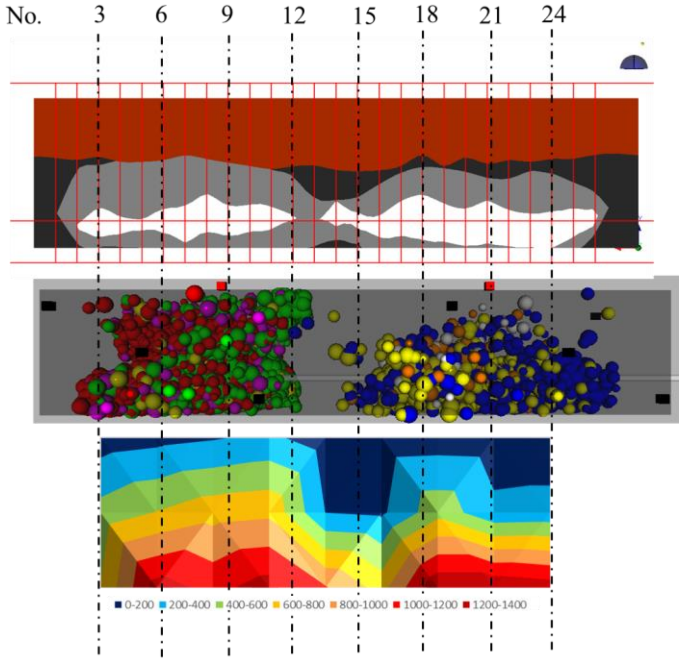

Fig. 23. Comparison of the combustion cavity and the temperature distribution of the section reconstruction and the calibration results of the AE source

3.3.3 Analysis of combustion cavity shape

In the process of UCG, when the temperature is higher than 400℃, the coal seam will react and form the corresponding gasification area, and when the temperature is higher than 800℃, the combustion cavity will be formed. The region where the two-dimensional temperature cloud map in Fig. 24 is higher than 800°C is the combustion cavity, and its shape is consistent with the shape of the cross-sectional reconstruction of the two-dimensional combustion cavity. Therefore, the temperature change in the gasifier can effectively and intuitively reflect the gasification process. The high-temperature area in the gasifier corresponds to the more intense area in the gasification reaction, reflecting the growth process of the combustion cavity.

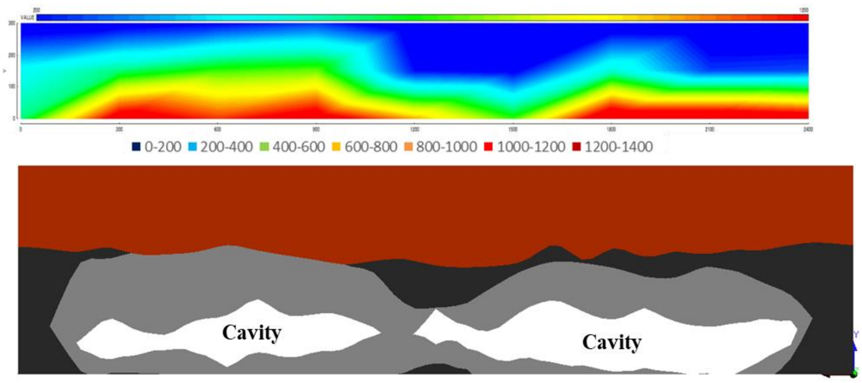

Fig. 24. Combustion cavity shape

3.4 3D construction of the gasification region and combustion cavity

Using the two-dimensional cross-sectional data of the 26 gasification zones and combustion cavities in Fig. 21, the three-dimensional shapes of the combustion cavity and the gasification zone are constructed, as shown in Fig. 25. In the horizontal coaxial UCG system, the gasification region is cylindrical with the gasification channel as the axis, and the radius of the cylinder increases with the increase in the degree of gasification. The cylinder on the left has an enormous volume, indicating the most violent degree of gasification. The cement filling layer around the middle of the gasification channel limits coal combustion, so the gasification area and combustion cavity are minimal. The gasification area on the right has a cement layer as an interlayer, which restricts the upward combustion of coal. Thus, the gasification area and combustion cavity are slightly smaller than those on the left. The concentrated area of AE source calibration and the high-temperature area in the coal seam are consistent with the fully expanded area of the constructed three-dimensional combustion cavity. According to the overall volume estimation by grid division, the combustion cavity is 50.774 cm^3, the gasification area is 237.007 $cm^{3,}$ and the artificial coal seam is 485.669 cm^3. The total amount of coal that fully underwent gasification was 10.5%; the total amount of coal that did not complete gasification was 48.8%.

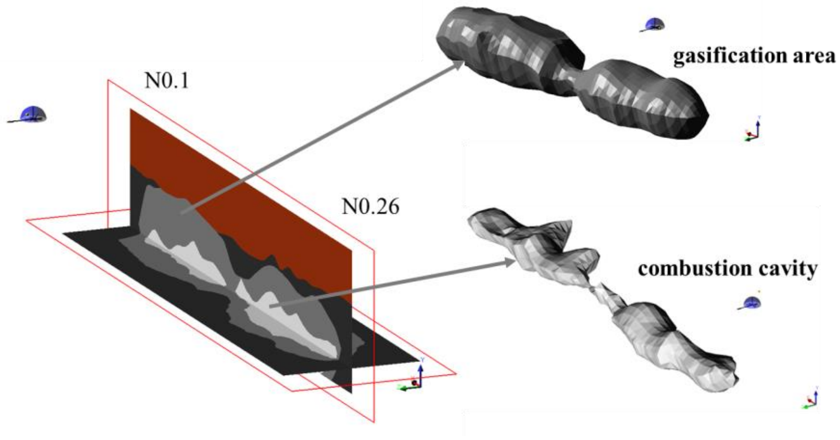

Fig. 25. 3D shapes of the combustion cavity and gasification zone

3.5 Product gas

Two methods were used to measure product airflow. One is to calculate the product gas flow through the nitrogen concentration. Assuming that all the nitrogen in the injected gasification agent is exhausted, the product gas flow is calculated according to the amount of injected nitrogen and the nitrogen concentration in the product gas analyzed by gas chromatography. The other measures the product gas flow during the experiment through an ultrasonic flowmeter. The comparison between the two is shown in Fig. 26. The ultrasonic flowmeter calculates the product gas flow according to the average movement of the gas. In contrast, once an hour, the nitrogen gas calculates the product gas flow according to the gas analysis's (instantaneous value) value. The two results show similar trends, indicating that the cavity's interior is stable, and the whole experiment has good airtightness.

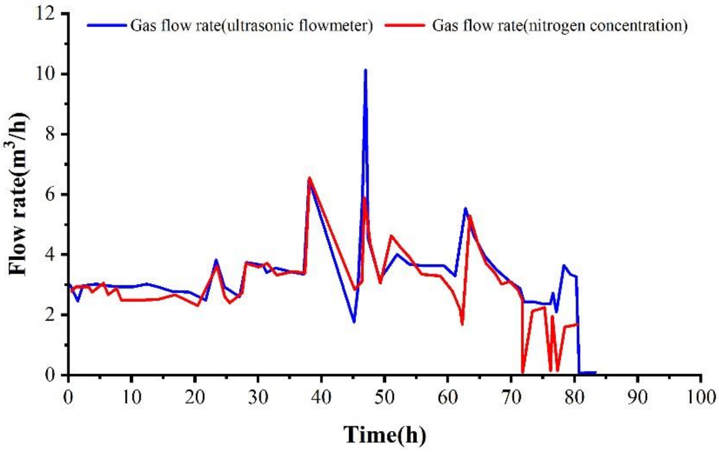

Fig. 26. Product gas flow

Fig. 27 shows the main components and calorific value of the product gas. The changing trend of the product gas composition is consistent with the monitoring results of the temperature sensor, and there are remarkable changes after the beginning of each stage. The combustible gases such as CO, H_2, and CH_4 increase sharply after the start of the test or after the port of the injection pipe is moved, and then gradually decrease. The calorific value of the product gas can be calculated according to the concentration of combustible gases such as H_2, CO, CH_4 and other hydrocarbons [30], and the change in the calorific value is the same as that of H_2, CO and CH_4. By moving the position of the injection tube port, the gasification area can be controlled to improve the calorific value of the product gas. When the quality of the product gas (flammable gas composition and calorific value) falls, the quality can achieve a sharp recovery by moving the filling pipe port, then gradually reducing the quality, and finally stabilized at 5MJ/Nm^3.

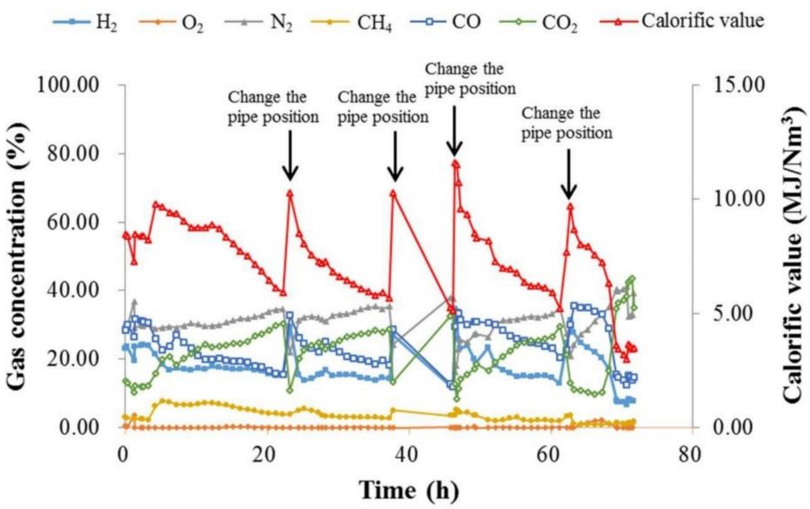

Fig. 27. Main compositions and the calorific value of product gas.

4 Conclusion

This paper used layered temperature monitoring and acoustic emission monitoring techniques to study the growth of the UCG combustion cavity in the horizontal coaxial gasification channel. After the experiment, the artificial coal seam was cut to obtain the section shape of the combustion cavity. Two-dimensional and three-dimensional gasification combustion cavities were constructed according to the profile shape, and were compared and verified with the monitoring results of temperature and acoustic emission. The main conclusions are summarized as follows:

In the gasification process of horizontal coaxial UCG, the nearby temperature rapidly rises with the movement of the injection pipe port, indicating that moving the injection pipe port can effectively guide the expansion direction of the gasification area. When the injection flow rate and composition of the gasification agent are the same, coal combustion is the most violent within four hours of the moving injection pipe. The local temperature exponentially increases, indicating that the combustion and gasification state is the most complete after four h of continuous ventilation.

The local temperature change is closely related to the AE activity in the gasifier. When the local temperature changes, the AE event gradually increases, and the movement of the AE source position is consistent with the movement of the high-temperature area. Combining the derivative movement in the high-temperature region and the AE source distribution, the combustion cavity's expansion process during the gasification process can be inferred. The calibration results of the AE source and the high-temperature derivation map in the horizontal coaxial UCG process are consistent with the 2D and 3D gasification combustion cavities reconstructed in the profile, indicating that AE and temperature monitoring can effectively infer the growth process of the gasification combustion cavity.

The horizontal coaxial UCG gasification zone is a cylinder with the channel as the axis, and the radius of the cylinder increases with the increase in the degree of gasification. This experiment has thick rock layers and cement interlayers in the middle of the gasification channel. Thus, the gasification area cannot be further expanded, indicating that the gasification process may be interrupted when large-scale gangue or collapsed columns appear in the coal seam during field production. In the profile X=1550 mm, a cement filling layer is approximately 10 mm wide in the upper left. However, the gasification area extends beyond this cement filling layer to the adjacent coal block, indicating that small-scale gangue has little influence on the gasification process.

Credit author statement

Fa-qiang Su: Investigation, Writing-Reviewing and Editing, Funding acquisition. Jun-bo Wu: Investigation, Writing-Original draft preparation, Funding acquisition. Tao-Zhang: Supervision, Validation. Qi-chao Deng: Investigation, Data curation. Akihiro Hamanaka: Conceptualization, Methodology. Yi-he Yu: Investigation, Validation, Data curation, Funding acquisition. Meng-jia Dai: Investigation, Validation. Jun-nan Yang: Validation, Resources. Xiao-long He: Investigation , Data curation.

Declaration of Competing Interest

The authors declare that they have no known competing financial interests or personal relationships that could have appeared to influence the work reported in this paper.

Acknowledgments

This work was supported by Key Laboratory of Western Mine Exploitation and Hazard Prevention, Ministry of Education (SKLCRKF1902), State Key Laboratory for Geomechanics and Deep Underground Engineering, China University of Mining & Technology (SKLGDUEK2004), Key R & D and promotion projects in Henan Province (222102320139), Henan Province Key Scientific Research Project Plan for Colleges and Universities (22B440003).

References

[1] Su Faqiang, Jing Shijie, Gao Xicai, Pu Hai, Fan Weitao, Yu Guanglei, Wu Junbo, Deng Qichao, Zhang Tao. Evaluation of combustion cavity development and energy recovery in underground coal gasification [J]. Coal Journal, 2021, 46(11): 3682-3691.

[2] Daggupati S,Mandapati R N,Mahajani R M ,et al. Laboratory studies on combustion cavity growth in lignite coal blocks in the context of underground coal gasification[J]. Energy, 2010, 35(6):2374-23867.

[3] Prabu V , Jayanti S . Simulation of cavity formation in underground coal gasification using bore hole combustion experiments[J]. Energy, 2011, 36(10):5854-5864.

[4] Wang F T , Mead S W , Stuermer D H . Groundwater contamination near the Hoe Creek UCG experiments. 1981.

[5] Wang F T , Mead S W , Stuermer D H . Mechanisms for groundwater contamination by UCG: preliminary conclusions from the Hoe Creek study. 1982.

[6] Raber E , Stone R . Ground-water hydrologic effects resulting from underground coal gasification experiments at the Hoe Creek Site near Gillette, Wyoming. Interim report, October 1979-March 1980. 1980.

[7] Mehdi, Najafi, Seyed, et al. Prediction of cavity growth rate during underground coal gasification using multiple regression analysis[J]. International Journal of Coal Science & Technology, 2015, 2(4):318-324.

[8] Nourozieh H , Kariznovi M , Chen Z , et al. Simulation Study of Underground Coal Gasification in Alberta Reservoirs: Geological Structure and Process Modeling[J]. Energy & Fuels, 2010, 24(MAY-JUN.):3540-3550.

[9] Pdf S . Modeling Cavity Growth in Underground Coal Gasification[J]. Journal of Energy, 2013, Vol. 7(no. 5):410-415.

[10] Chen, Liang~a, Hou, et al. A back analysis of the temperature field in the combustion volume space during underground coal gasification[J]. Mining Science and Technology, 2011.

[11] Perkins G , Sahajwalla V . A Numerical Study of the Effects of Operating Conditions and Coal Properties on Cavity Growth in Underground Coal Gasification[J]. Energy & Fuels, 2006, 20(2):81 - 88.

[12] Luo Y, Coertzen M, Dumble S. Comparison of UCG cavity growth with CFD model predictions. In: Proceedings of the 7th international conference on CFD in the minerals and process industries CSIRO, melbourne, Australia; December 2009. p. 9e11.

[13] Seifi M, Chen Z, Abedi J. Numerical simulation of underground coal gasification using the CRIP method. Can J Chem Eng 2011;89(6):1528-35

[14] Samdani G, Aghalayam P , Ganesh A , et al. A process model for underground coal gasification – Part-I: Cavity growth[J]. Fuel, 2016.

[15] Samdani G , Aghalayam P , Ganesh A , et al. A process model for underground coal gasification – Part-II growth of outflow channel[J]. Fuel, 2016, 181:587-599.

[16] Sarndani G , Aghalayam P , Ganesh A , et al. A process model for underground coal gasification – Part-III: Parametric studies and UCG process performance[J]. Fuel, 2018, 234(DEC.15):392-405.

[17] Aj A ,Fs A ,Mn B . A new model for evaluation of cavity shape and volume during Underground Coal Gasification process - ScienceDirect[J]. Energy, 2018, 148:756-765.

[18] G. J , Harloff. Underground Coal Gasification Cavity Growth Model[J]. Journal of Energy, 1983.

[19] Daggupati S , Mandapati R N , Mahajani S M , et al. Laboratory studies on cavity growth and product gas composition in the context of underground coal gasification[J]. Energy, 2011, 36(3):1776-1784.

[20] Yang Lanhe, Liang Jie. TEM detection method in the combustion air area of underground coal gasification [J]. Journal of Nanjing University of Science and Technology, 2001, 25(2):5.

[21] Chen Qihui, Liang Jie, Yu Li, et al. Research on detection of underground gasification combustion zone and moving speed by radon measurement method [J]. Journal of Shandong Jianzhu University, 2008, 24(3):5.

[22] Jinghua Liu, Xingtai Wang, Gang Tian, Zhuwen Wang. Dynamic monitoring of coal underground gasification goafs by radioactive radon measurement [J]. Geophysical and Geochemical Exploration,2000(02):92-98.

[23] Najafi M , Jalali S , Khalokakaie R , et al. Prediction of cavity growth rate during underground coal gasification using multiple regression analysis[J]. International Journal of Coal Science & Technology, 2015, 2(004):318-324.

[24] Prabu V , Jayanti S . Simulation of cavity formation in underground coal gasification using bore hole combustion experiments[J]. Energy, 2011, 36(10):5854-5864.

[25] Prabu V , Jayanti S . Heat-affected zone analysis of high ash coals during ex situ experimental simulation of underground coal gasification[J]. Fuel, 2014, 123(may 1):167-174.

[26] Jowkar A , Sereshki F , Najafi M . Numerical simulation of UCG process with the aim of increasing calorific value of syngas[J]. International Journal of Coal Science & Technology, 2020, 7(1):196-207.

[27] Javed S B , Uppal A A , Bhatti A I , et al. Prediction and parametric analysis of cavity growth for the underground coal gasification project Thar[J]. Energy, 2019, 172(APR.1):1277-1290.

[28] Su F Q , Itakura K I , Deguchi G , et al. Monitoring of coal fracturing in underground coal gasification by acoustic emission techniques[J]. Applied Energy, 2017, 189(MAR.1):142-156.

[29] Su F Q , Hamanaka A , Itakura K I , et al. Monitoring and evaluation of simulated underground coal gasification in an ex-situ experimental artificial coal seam system[J]. Applied Energy, 2018, 223(AUG.1):82-92.

[30] Yang Lanhe. Research on the characteristics and influencing variables of the "three zones" of underground coal gasification [J]. Journal of Nanjing University of Science and Technology (Natural Science Edition), 2001(05):533-537.DOI:10.14177/j. cnki.32-1397n.2001.05.021.

[31] Ekneligoda T C , Marshall A M . A coupled thermal-mechanical numerical model of underground coal gasification (UCG) including spontaneous coal combustion and its effects[J]. International Journal of Coal Geology, 2018, 199:31-38.

[32] Xu B , Yang M , Xing B , et al. Removal of pollutants from aqueous solutions by coals and residual cokes obtained from simulated underground coal gasification experiments[J]. Fuel, 2021, 292(4):120292.

[33] Ma Ailing, Chen Lunjian, Xu Bing. Study on the physicochemical properties of residues in the "three belts" of underground coal gasification [J]. Coal Science and Technology, 2019, 47(11): 217-223. DOI: 10.13199/j .cnki.cst.2019.11.031